January 2012

Effects of Random Cross-Sectioned Distributions, Fiber Misalignment and Interphases in Three-Dimensional Composite Models on Transverse Shear Modulus

Jarrett Zitko
University of South Florida, jzitko@engineer.com

Effects of Random Cross-Sectioned Distributions, Fiber Misalignment and Interphases in Three-Dimensional Composite Models on Transverse Shear Modulus

by

Jarrett Albert Zitko

A thesis submitted in partial fulfillment
of the requirements for the degree of
Master of Science in Mechanical Engineering
Department of Mechanical Engineering
College of Engineering
University of South Florida

Major Professor: Autar Kaw, Ph.D.
Craig Lusk, Ph.D.
Ali Yalcin, Ph.D.

Date of Approval:
June 18, 2012

Keywords: Polar Fiber Orientation, Random Fiber Arrangement, Halpin-Tsai, Scale, Mesoscale Window, Elastic Moduli, Composite Materials

DEDICATION

This thesis is dedicated to my parents whose loving care and wisdom have given me the inspiration and confidence to reach my goals. To my father, Dwaine Zitko and his wife Ursula Zitko, as well my grandparents Barbara and Albert Navas, who gracefully provided the needed financial support. To my wife Dominique, who has supported and cheered me on throughout my academic endeavors. To my professor, Dr. Kaw, who provided meaningful insight and guidance throughout my research.

ACKNOWLEDGMENTS

I would like to acknowledge the many contributions that I have received relevant to my research work, both directly and indirectly. Particularly, I would like thank Dr. Yalcin and Dr. Lusk for taking time to serve on my supervisory committee, and Dr. Kaw, for his continued guidance and the resources he provided.

Furthermore, I would like to thank my parents for their unwavering support and guidance that helped me grow into the person I am today. My father summarized the proper approach to success pointedly by saying: "Don't follow dreams, as dreams are unattainable. Instead view a dream as a goal and follow it vehemently, because a goal can be achieved with thoughtful planning." I would also like to acknowledge my wife Dominique, who provided me with timely acts of encouragement, comfort, and wisdom when I needed it the most.

Lastly, I would like to acknowledge individual contributions from fellow graduate student Sri Garapati, whose knowledge of ANSYS software and general university procedures proved helpful in the completion of my work.

This research has been supported in part by the University of South Florida.

TABLE OF CONTENTS

LIST OF TABLES

LIST OF FIGURES

ABSTRACT

Finite element analysis was implemented to evaluate the transverse shear modulus of a unidirectional glass/epoxy fiber-matrix composite based on pure shear displacement boundary conditions. Unit cells consisting of three-dimensional glass cylinders surrounded in square-cuboid epoxy matrices were modeled to represent "Representative Volume Element" (RVE) configurations in periodic and random-periodic square cell arrangements of variable size. Three RVEs were constructed and analyzed: A single unit cell, a 9-cell (3 x 3) array, and a 25-cell (5 x 5) array. Additionally, the unit cell was modeled to include an interphase. Three sets of cell arrangements were constructed and evaluated: a periodic square array, a transversely distributed random-periodic array, and a variable angularly aligned random-periodic array. Furthermore, scale and free-edge effects of the composites were studied by evaluating the shear modulus in incrementally increasing domains, as well as by isolating finite-sized domains called windows within the multiple-cell model, whereby the window is smaller than the array. Finite element software was subsequently utilized to create a three-dimensional mesh of the composite models studied. Each simulation consisted of exposing the respective domain to pure shear boundary conditions, whereby the model was subject to uniform transverse displacement along its boundary. Subsequent volumetric averaging resulted in computation of the apparent transverse shear modulus. The resulting numerically attained elastic shear modulus was then evaluated and compared to known predictive models in literature. It was shown that that the transverse random

arrangement as well the random angular alignment of fibers within the composite structure had a marginal influence on the shear modulus. For random transverse distributions, a deviation in modulus of +1.5% was observed for the 25-cell array as compared to a periodic array of equal size. Similarly, a deviation of +0.3% was predicted for 25-cell arrays subject to random angular fiber misalignments up to ±0.143°, as compared 25-cell periodic arrays. Furthermore, increasing the composite medium by systematic, incremental augmentation model domains was shown to significantly lower the shear modulus in a convergent manner as G_{23} values dropped 33.5% from the nonhomogeneous single cell to the 9-cell model, and 2.6% from the same 9-cell to the 25-cell model, while observing the effects of a mesoscale window displayed little variance in modulus value as compared to the larger RVE from which the window was isolated from. Lastly, the predictive potential of the model developed by Sutcu for composites with interphases, and other commonly employed models for predicting the transverse shear modulus of unidirectional composites was also evaluated. Numerical results of nonhomogeneous interphase models for both periodic and random-periodic 25-cell arrays were found to be in excellent agreement with Sutcu's approximation. The shear modulus of the 25-cell, nonhomogeneous interphase model was found to lie within 3.5% of Sutcu's prediction. Volume averages for periodic arrays with no interphase were observed to lie in close proximity to Halpin-Tsai's model, displaying a variation of 7% for a 25-cell, single fiber model.

CHAPTER 1 LITERATURE REVIEW

1.1 Introduction

Current mechanical and structural designs made of low density, strong, and stiff composite bodies bring forth the need for accurate prediction of equivalent elastic properties. While elaborate and often expensive experimental testing techniques exist today, it is often required to attain accurate approximations of the elastic properties of a composite in early to middle stages of engineering design, prior to committing to experimental validation through testing of a sample specimen in the final stages of design.

An abundance of research has been devoted to obtaining predictions of equivalent moduli of composite media. Analytical solutions using classic elastic theory resulted in widely accepted models for obtaining the elastic moduli of unidirectional composites. However, much debate still exists on recent efforts in predictions involving the transverse shear modulus of composite materials (see Hashin [23], for example). Thenceforth, a brief literature review of common approximation models is presented and discussed here.

A majority of materials used in engineering design and mechanical/structural assembly fall into two major categories: Isotropic and Orthotropic materials. Such materials are either homogeneous or nonhomogeneous. A homogeneous material has identical physical properties at any point in a body, whereas a nonhomogeneous material exhibits physical properties as a function of position within the body. An isotropic material possesses identical properties in all directions along a globally

defined coordinate system. For example, consider the isotropic solid block in Figure 1.

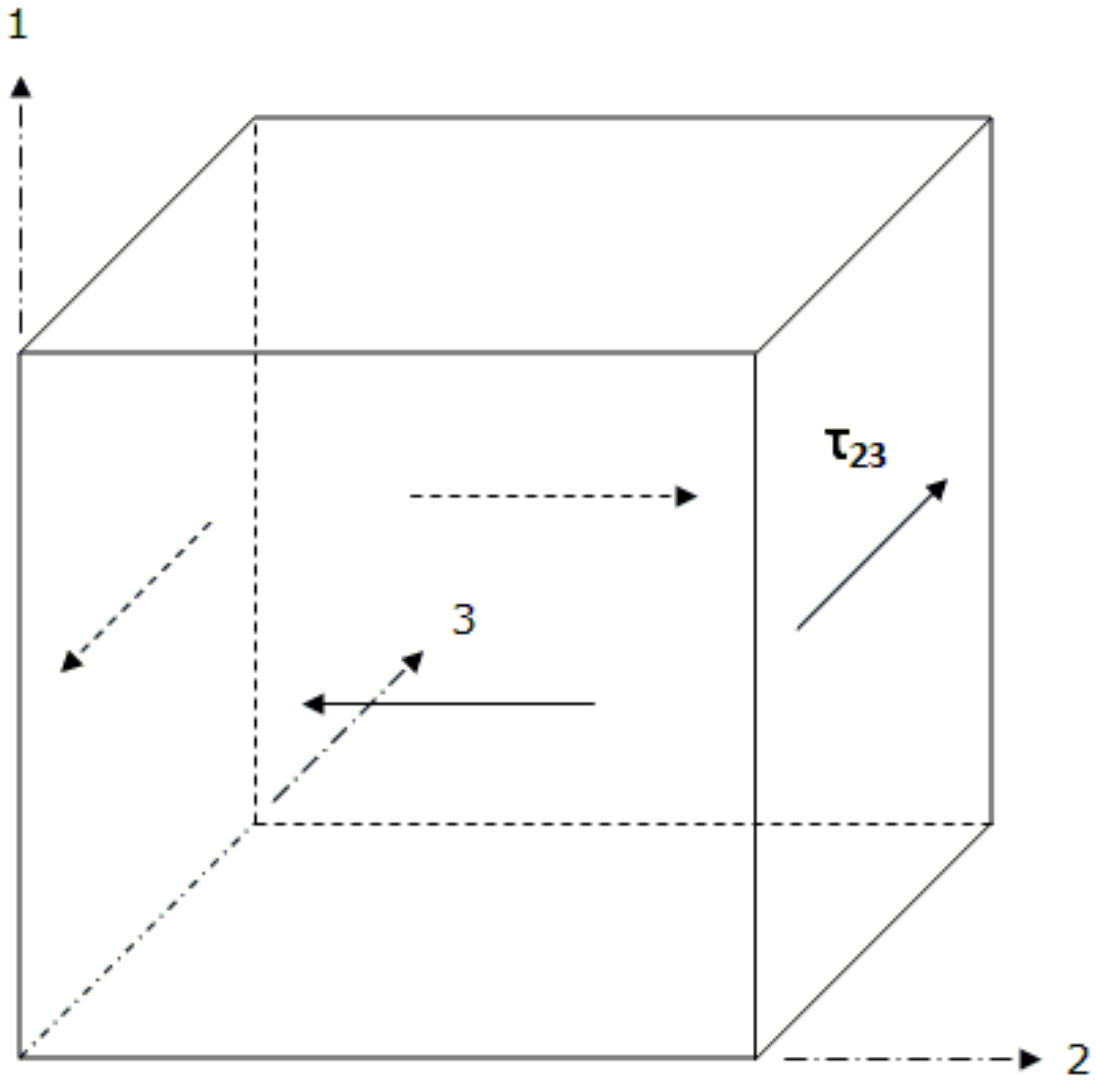

Figure 1 – Isotropic Solid Cuboid Subject to Pure Shear Loading

The global coordinate system is defined by the 1, 2, and 3 axes, respectively. In this solid, all physical properties are the same in all three coordinate directions.

An important class of physical properties in engineering analysis is elastic moduli. For bodies that are considered linear elastic and subject to only small deformations, the displacements, stresses, and strains within such bodies are defined by Hooke's Law, compatibility conditions, and force equilibrium equations as 15 unknown parameters at any point in a homogeneous body [19]. For linearly isotropic materials the aforementioned constants are defined solely by Young's modulus E and Poisson's ratio ν. The shear modulus G of an isotropic solid is a function of both E and ν, and is defined by the expression:

$$G = \frac{E}{2(1+\nu)} \tag{1}$$

Consider the cuboid solid in Figure 1 subject to a state of pure shear loading, whereby a shear stress of τ_{23} is applied to 2-3 plane as shown. Correspondingly, the shear modulus may also be expressed by the stress-strain relation:

$$G = \frac{\tau_{23}}{\gamma_{23}} \tag{2}$$

where τ_{23} and γ_{23} denote the shear stress and shear strain in the 2-3 plane, respectively. It is of importance to note here that the shear modulus is the same in all planes for isotropic materials, i.e. $G_{23} = G_{31} = G_{12} = G$.

Orthotropic materials, on the other hand, consist of "three mutually perpendicular planes of material symmetry" [19]. Thus, an orthotropic material has identical elastic properties in all directions in three mutually perpendicular planes, respectively [19]. In this case, the 15 unknown parameters in a linearly elastic body

are defined by nine independent elastic constants [19]. Figure 2 shows an example of an orthotropic body.

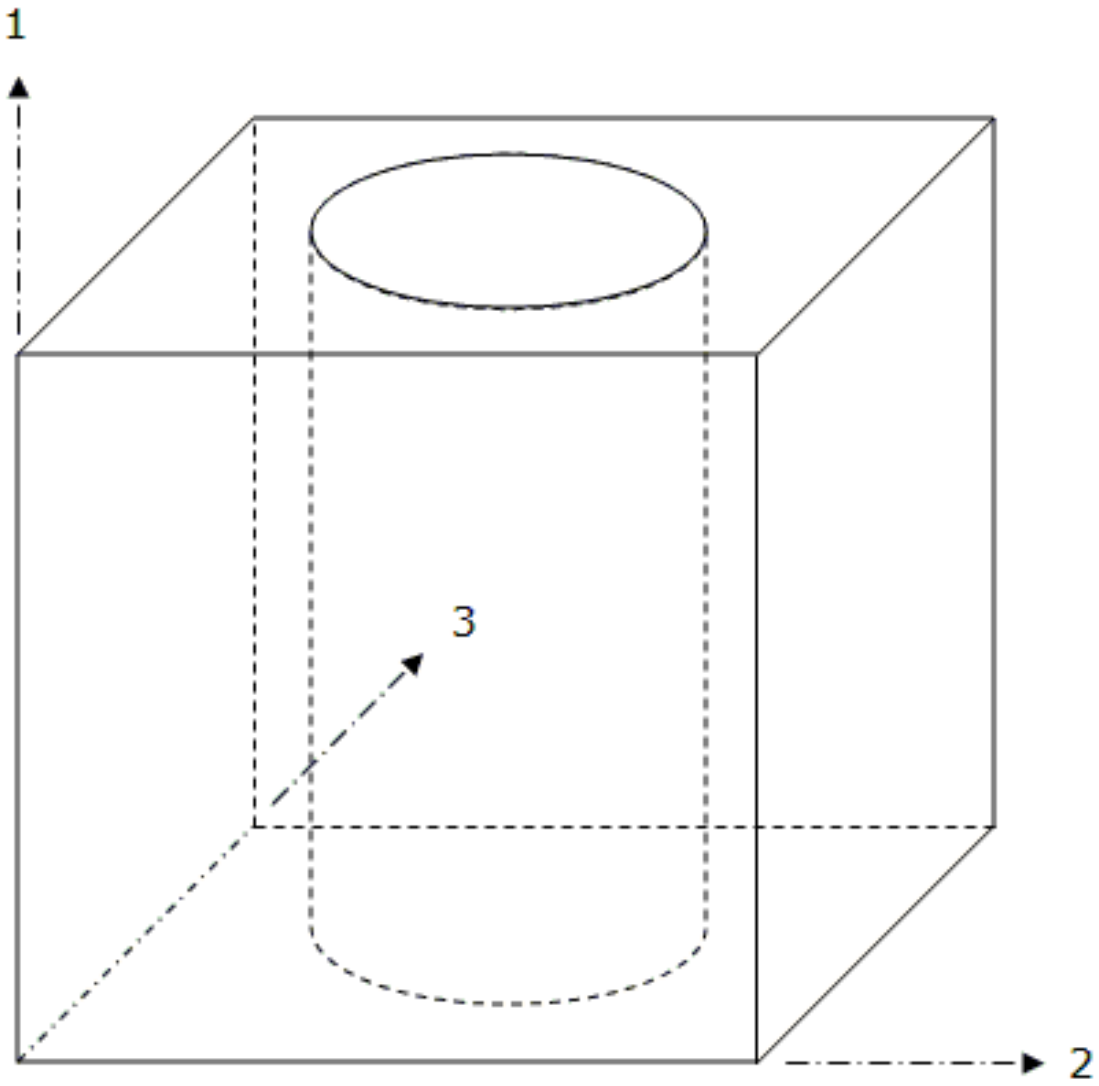

Figure 2 – Unidirectional Fiber Composite (Orthotropic Material)

Figure 2 describes a single composite body consisting of a continuous cylindrical fiber that is embedded in a square cuboid material called the matrix, which is dissimilar from the fiber material. Both individual constituent materials in

this example are isotropic; however, such composite laminated materials may also be comprised of transversely isotropic phase materials. An example of a composite consisting of isotropic constituents is a glass/epoxy composite [19]. Conversely, an example of a composite consisting of an isotropic matrix with transversely isotropic fibers is a graphite/epoxy composite body. Further distinction can be made with orthotropic materials with uniaxially aligned fiber composites, as such bodies exhibit identical elastic properties in the two directions perpendicular to the fiber [19]. Such materials are considered transversely isotropic. Resultantly, the shear moduli in the 1-2 and 1-3 are identical; however, the shear modulus in the 2-3 plane is not. Thus, distinction is made between the so called longitudinal shear modulus $G_{12} = G_{13}$, and the transverse shear modulus G_{23}.

1.2 Predictive Models of Transverse Shear Modulus of Fiber Reinforced Composites

As a preface to presenting the findings of the subject at hand, it is necessary to review and discuss relevant predictive models that can be found in literature today. We begin our discussion with a brief review of the Halpin-Tsai [1] and Christensen [2] models for predicting the transverse shear modulus of unidirectional composites with no interphase, followed by Sutcu's approximation which includes considerations of fiber reinforced composites with multiple interphases. Central to the discussion will be the inherent complexity in determining an exact deterministic theoretical value of the aforementioned elastic constant. Subsequent discussion will then focus on comparing the results of finite element method (FEM) models developed for this thesis to the aforementioned approximations. Indeed, if it is possible to confirm the accuracy and applicability of pertinent theoretical models, it would improve the efficiency in designing mechanical and structural composite bodies. Moreover, it would be of great benefit to design engineers and researchers

alike to achieve accurate modulus values numerically using finite element modeling and analysis techniques. The goal is to validate predictive modulus values found in literature as well as develop a more involved and complex finite element simulation models for determining the transverse shear modulus of a macroscopically homogenous unidirectional composite subject to variation of its geometric parameters.

1.2.1 Halpin-Tsai Model

The first approximation discussed is the Halpin-Tsai model [1]. The Halpin-Tsai equations are based on a semi-empirical model that utilizes curve fitting of an undetermined parameter to experimental data. Specifically, in addition to the fiber and matrix elastic moduli, the fitted parameter varies according to the geometric cross-section, packing distribution, and orientation of the fiber within the matrix. Halpin-Tsai [1] mentions that the micromechanics employed in this approach are based upon the Self-Consisted Method (SCS) first developed by Hill [24]. "Halpin and Tsai subsequently reduced Hill's results to a simpler analytical form and extended its use to a variety of reinforcement geometries" [1].

Hill [24] modeled the composite as a single fiber, enveloped in a cylindrical matrix that is embedded in an infinitely large homogeneous medium, as shown in Figure 3. It is important to note that "homogeneous medium" implies that the composite is considered macroscopically or statistically homogeneous; this means that all global geometrical characteristics such as fiber and matrix volume fractions are the same for any Representative Volume Element (RVE). A RVE describes a three-dimensional unit cell consisting of two unidirectional and concentric cylinders, where the cylindrical fiber is enclosed by a cylindrical matrix as is displayed in Figure 3.

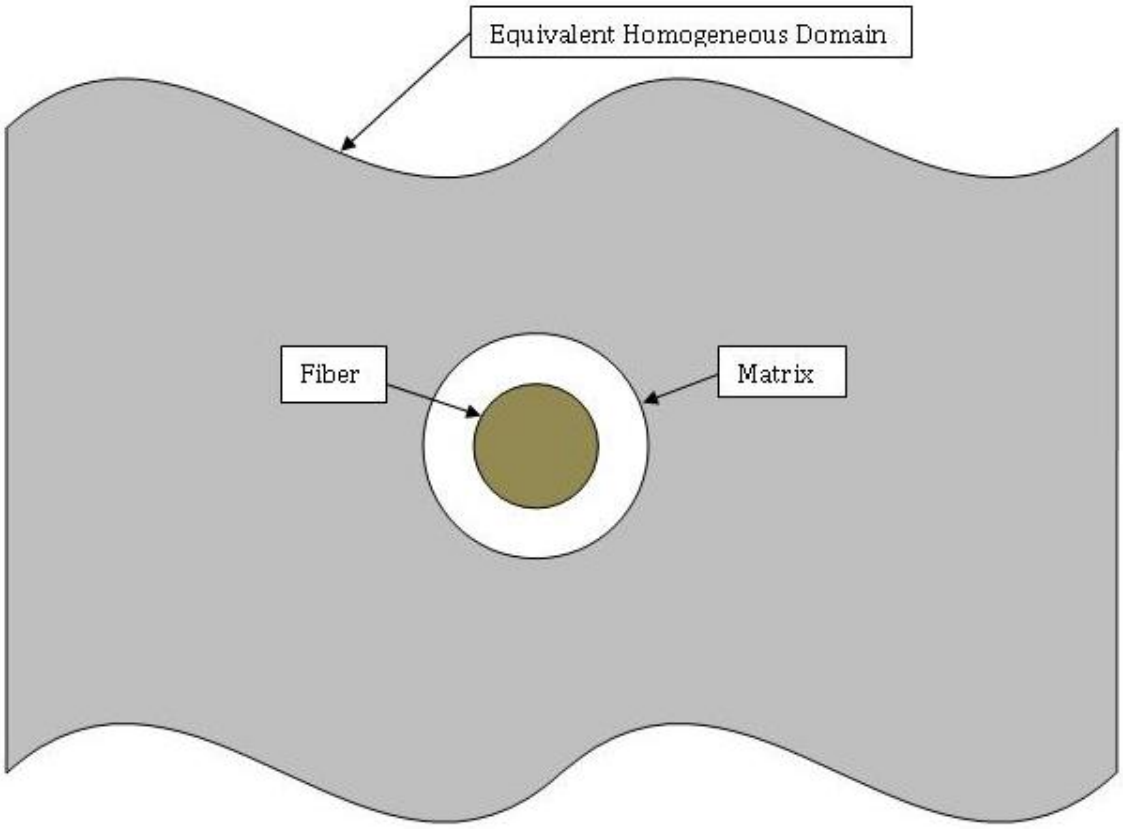

Figure 3 – Halpin-Tsai Self-Consistent Scheme (SCS) Model

However, complexity arises with the SCS model for determining the transverse shear modulus G_{23}. The boundary conditions on the homogeneous medium are one of pure shear loading such that

$$\tau_{xy} = \tau^0 = \text{constant} \tag{3}$$

with all other stresses vanishing, as rearticulated by Whitney and McCullough [5]. τ_{xy} is defined identically as is displayed in Figure 1, with the exceptions being that the shear stress refers to xyz axes in lieu of the 123 coordinate system, and the

shear stress is applied at an infinite distance from the matrix in the equivalent homogeneous medium (referring to Figure 3). Equation (3) leads to the following surface stresses for both the homogeneous medium and the composite cylinders. Rewriting Equation (3) in polar form we get

$$\sigma_r^0 = \tau^0 \sin 2\theta \tag{4a}$$

$$\tau_{r\theta}^0 = \tau^0 \cos 2\theta \tag{4b}$$

where σ_r and $\tau_{r\theta}$ are related to the Cartesian coordinate system as depicted in Figure 4.

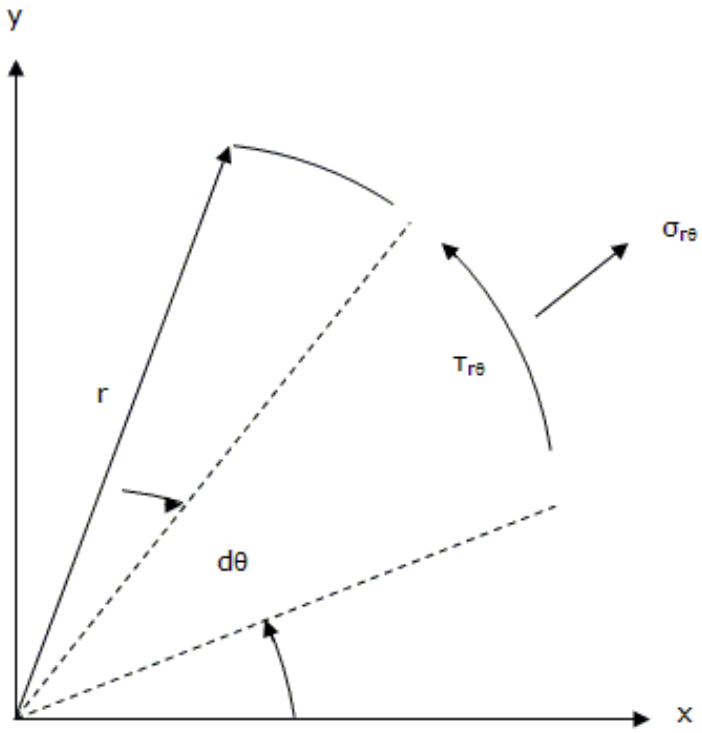

Figure 4 – Shear Stress Components in Polar Coordinates

Note that the z axis (into the page) in Figure 4 is omitted for clarity. Additionally, both cylinders are assumed to be in a state of plane strain such that

$$u_z = 0,\ u_r = u_r(r,\theta),\ u_\theta = u_\theta(r,\theta) \qquad (5a - c)$$

where u_z, u_r, and u_θ define the displacements in the z, r, and θ directions. The set of differential equations emerging from elastic theory which must satisfy conditions of continuity, compatibility, equilibrium of forces, and Hooke's Law cannot be satisfied simultaneously because each equation produces a different expression for G_{23}. In other words, a unique solution does not exist. This is to be interpreted physically that the continuity conditions between the RVE and the homogeneous medium are not completely satisfied. Thus, the SCS model is incapable of determining the value of G_{23}. This led to a modification of the original SCS model by Hermans [20] that was later adopted by Halpin [1] who assumed that the average transverse shear modulus of a free concentric cylinder subject to arbitrary surface stresses provides a reasonable estimate of G_{23}. More specifically, strain and stress is assumed constant within the boundaries of the cylindrical fiber inclusion. Thus, Equations (4a) and (4b) are altered slightly such that (per [5]):

$$\sigma_r^0 = A\sin 2\theta \qquad (6a)$$

$$\tau_{r\theta}^0 = B\cos 2\theta \qquad (6b)$$

where A and B are arbitrary constants. These boundary conditions along with assumption of plane strain led to the equation for the transverse modulus G_{23} (upon solving the force equilibrium equations) as formulated by Chow and Hermans [20] in its final form as

$$\bar{G}_{23} = G_m \frac{2V_f G_f (k_f + G_m) + 2V_m G_m + V_m k_m (G_f + G_m)}{2V_f G_m (k_f + G_m) + 2V_m G_f G_m + V_m k_m (G_f + G_m)} \qquad (7)$$

where the subscripts f and m denote the fiber phase and matrix phase, respectively, and

- $\bar{G}_{23}$ = Equivalent transverse shear modulus of composite cylinder
- V_i = Volume fraction of phase constituent
- G_i = Shear modulus of phase constituent
- k_i = Plane strain bulk modulus of phase constituent
- i = f for fiber and m for matrix

It should be further clarified that the bulk modulus k_i of the phase constituent under longitudinal plane strain is

$$k_i = \frac{E_i}{2(1+\nu_i)(1-2\nu_i)} \tag{8}$$

where E_i and ν_i denote the Young's modulus and Poisson's ratio of the constituents, respectively. Halpin-Tsai's rearticulation of Hermans' Equation (7) incorporated the term ζ, called the reinforcing factor, which depends on fiber geometry, packing geometry, and loading conditions. Reliable estimates for ζ can be obtained by comparison of the Halpin-Tsai equation with numerical micromechanical solutions. The reinforcement parameter for the transverse shear modulus $\bar{G}_{23}$ for a circular fiber embedded in a square array is

$$\zeta = \frac{k_m/G_m}{(k_m/G_m)+2} \tag{9}$$

Thereafter, Equation (7) may be rearranged to incorporate ζ as follows

$$\bar{G}_{23} = G_m \frac{1 + \zeta\eta V_f}{1 - \eta V_f} \tag{10}$$

where

$$\eta = \frac{(G_f/G_m) - 1}{(G_f/G_m) + \zeta} \tag{11}$$

Ensuing research publications [1, 23] invalidate Hermans' [20] and therefore Halpin-Tsai's approximation [1] of the transverse shear modulus on the basis that Hermans mistakenly assumed that the state of strain in the fiber phase is uniform. However, numerous published experimental and numerical results (see [12], for example) are in acceptable agreement with Halpin-Tsai's approximation. Thus, the Halpin-Tsai equation is still widely employed in composite design.

1.2.2 Christensen Model

Christensen and Lo [2] extended the SCS model to include a third, outer cylindrical phase composed of an equivalent homogeneous material to predict the effective approximation of the transverse shear modulus of a transversely isotropic composite. In his work, Christensen sought to address Hermans' assumption that the "state of stress in the fiber phase is uniform in shear" [2], as briefly discussed in Section 1.2.1. The Christensen model is depicted in Figure 5.

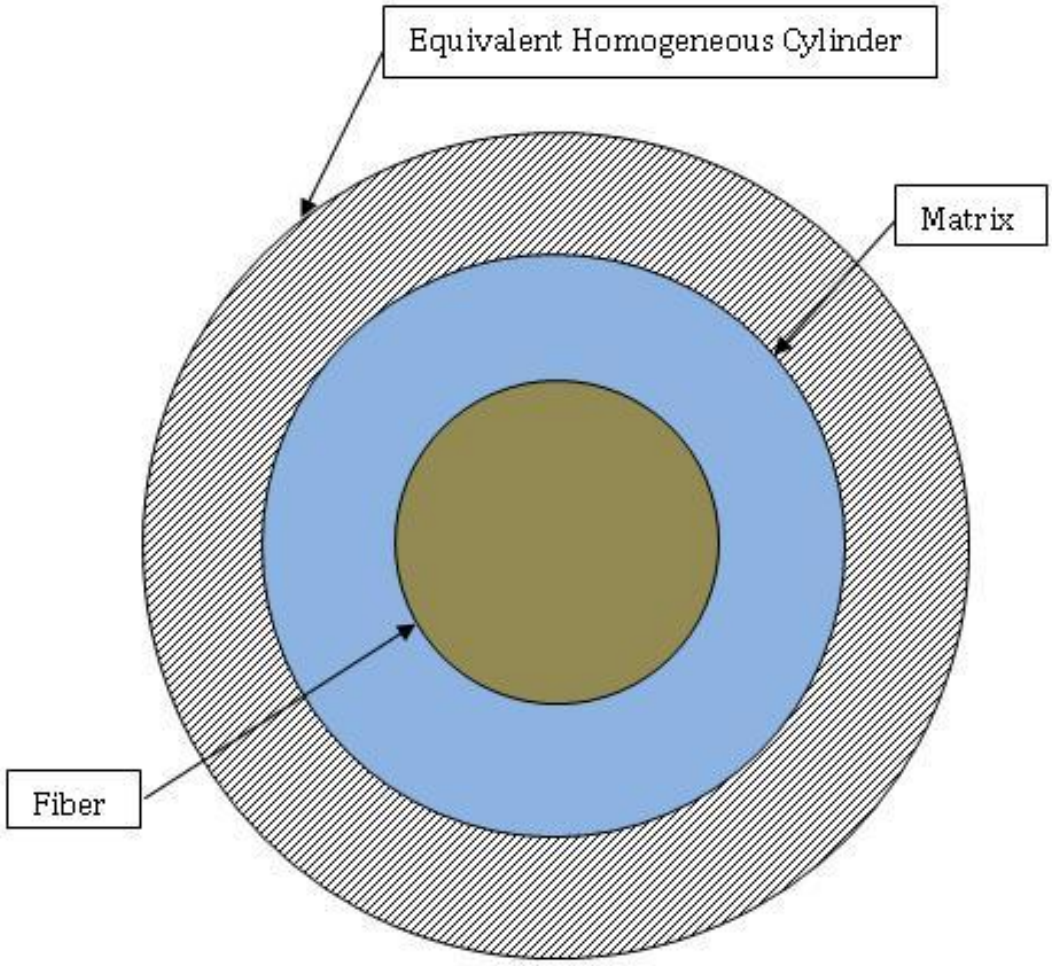

Figure 5 – Three-Phase Model of a Fiber-Matrix Composite RVE

Similar to the generalized SCS, the model consists of a composite cylinder surrounded in an infinite, macroscopically homogeneous medium, whereby the equivalent cylinder possesses the same average properties as the fiber-matrix composite. To determine the transverse shear modulus, Christensen made use of the expression for strain energy U which represents the total strain energy stored in the model. The goal is to solve for G_{23} of an equivalent homogeneous medium, such that the homogeneous cylinder stores the same amount of energy U as the fiber-

matrix composite. Utilizing energy equivalency relations, the energy statement carries the final form

$$\int_0^{2\pi} [\sigma_r^0 u_{re} + \tau_{r\theta}^0 u_{\theta e} - \sigma_{re} u_r^0 - \tau_{r\theta e} u_\theta^0]_{r=b} b d\theta = 0 \qquad (12)$$

where

- σ_r^0 = Normal Stress at infinity in the homogeneous medium
- $\tau_{r\theta}^0$ = Shear Stress at infinity in the homogeneous medium
- u_i^0 = Displacement at infinity in the homogeneous medium ($i = r, \theta$)
- $\sigma_{r\theta}^0$ = Normal Stress of equivalent homogeneous medium ($i = r, \theta$)
- u_{ie} = Displacement of equivalent homogeneous medium ($i = r, \theta$)

As with Halpin's [1] relations in Equations (5a - c), plane strain conditions are assumed. Assuming conditions of simple shear at infinity in the homogeneous medium, it follows that

$$\sigma_r^0 = \cos 2\theta \qquad (13a)$$

$$\tau_{r\theta}^0 = -\sin 2\theta \qquad (13b)$$

Successive calculations determined from the conditions of compatibility, continuity, equilibrium of forces, and Hooke's Law gives the following stresses and displacements as a function of r and θ of the equivalent homogeneous cylinder:

$$u_{re} = u_{re}(r, \theta) \qquad (14a)$$

$$u_{\theta e} = u_{\theta e}(r, \theta) \tag{14b}$$

$$\sigma_{re} = \sigma_{re}(r, \theta) \tag{14c}$$

$$\tau_{r\theta e} = \tau_{r\theta e}(r, \theta) \tag{14d}$$

Substituting well known relations of elastic constants for unknown constants in Equation (12), along with replacement of these newly derived relations in Equations (13a - b) gives the governing quadratic equation for the effective transverse shear modulus G_{23} as:

$$\left(\frac{G_{23}}{G_m}\right)^2 \cdot A + \left(\frac{G_{23}}{G_m}\right) \cdot B + D = 0 \tag{15}$$

where A, B, and D [2] are given by:

$$A = 3f_i(1-f_i)^2(\alpha_1 - 1)(\alpha_1 + \alpha_2) + [\alpha_1\alpha_3 + \alpha_2\alpha_3 - (\alpha_1\alpha_3 - \alpha_2)f_i^3]$$

$$\cdot[f_i\alpha_3(\alpha_1 - 1) - (\alpha_1\alpha_3 + 1)] \tag{16}$$

$$B = -3f_i(1-f_i)^2(\alpha_1 - 1)(\alpha_1 + \alpha_2) + 1/2 \cdot [\alpha_3\alpha_1 + (\alpha_1 - 1)f_i + 1] \cdot [(\alpha_3 - 1)(\alpha_1 + \alpha_2)$$

$$- 2(\alpha_1\alpha_3 - \alpha_2)f_i^3] + \frac{f_i}{2}(\alpha_3 + 1)(\alpha_1 - 1) \cdot [\alpha_1 + \alpha_2 + (\alpha_1\alpha_3 - \alpha_2)f_i^3] \tag{17}$$

$$C = 3f_i(1-f_i)^2(\alpha_1 - 1)(\alpha_1 + \alpha_2) + [\alpha_3\alpha_1 + (\alpha_1 - 1)f_i + 1] \cdot [\alpha_1 + \alpha_2 + (\alpha_1\alpha_3 - \alpha_2)f_i^3] \tag{18}$$

and α_1, α_2, α_3, and f_i [2] are defined as

$$\alpha_1 = \frac{\bar{G}_{j-1}}{G_i} \tag{19}$$

$$\alpha_2 = 1 + \frac{2\bar{G}_{j-1}}{\bar{k}_{j-1}} \tag{20}$$

$$\alpha_3 = 1 + \frac{2G_i}{k_i} \tag{21}$$

$$f_i = \left(\frac{r_{i-1}}{r_i} \right)^2 \text{, and} \qquad (22)$$

r_i = radius of i^{th} constituent phase, and r_{i-1} = radius of $(i-1)^{th}$ constituent phase.

Additionally the following terms are defined as

- $\bar{G}_{j-1}$ = Transverse Shear Modulus of the $(j-1)^{th}$ equivalent homogeneous cylinder (j = 1,…,n and j = 1 is the first homogeneous cylinder following the innermost fiber phase)
- G_i = Transverse Shear Modulus of the i^{th} constituent phase
- $\bar{k}_{j-1}$ = Plane Strain Bulk Modulus of the $(j-1)^{th}$ equivalent homogeneous cylinder (j = 1,…,n and j = 1 is the first homogeneous cylinder following the innermost fiber phase)
- k_i = Plane Strain Bulk Modulus of the i^{th} constituent phase

1.3 Predictive Models of Transverse Shear Modulus for Fiber with Interphase

During the manufacturing of composites with cylindrical inclusions, a bonding reaction transpires through a diffusion process at the fiber-matrix boundaries. As a result, marked by transition zone between both constituent materials, an interfacial layer called the interphase is created (see Figure 6). Several authors have developed micromechanical models for studying the elastic behavior of continuous fiber-reinforced composites with inclusion of an interphase. Wacker, et. al. [22] suggested that such an interphase is nonhomogeneous where the interphase has "elastic properties which are changing with the radial distance from the fiber boundary" [22]. Interphase layers may also be intentionally introduced to alter the

mechanical properties of the composite. These coatings may be either homogeneous, that is consisting of uniform elastic properties throughout the volume of the interphase, or nonhomogeneous [4]. In another study, Garapati [4] assumed that the "interphase region might have multiple regions of chemically distinct layers" [4], which essentially describes a quasi nonhomogeneous region consisting of discrete homogeneous layers. Delale and Erdogan [6], Erdogan [7], and Kaw, et. al. [8] developed micromechanics models with nonhomogeneous interphases in which the elastic moduli of the interphase was assumed to vary exponentially along the radial thickness of the interphase. Bechel and Kaw [8] modeled the interphase as an arbitrary piecewise continuous function along the thickness of the annular-cylindrical inclusion. The latter model by Bechel and Kaw [8] is adopted in the approximation model of this study.

Garapati [4] provided mathematical models for calculating the elastic moduli of an interphase region that varies both linearly and exponentially along the radial thickness of the interphase layer. A symbolic representation of the interphase region along with relevant description of terms is shown in Figure 6.

The model adopted in this paper includes an interphase model for which the elastic moduli vary linearly through the radial distance. Garapati developed the case of linearly varying elastic moduli along the radial thickness in which the Young's modulus and Poisson's ratio are given by:

$$E(r) = a + br, \text{ for } r_f \le r \le r_i \tag{23}$$

and

$$\nu(r) = c + dr, \text{ for } r_f \le r \le r_i \tag{24}$$

where a,b,c, and d are determined by substituting values of E and ν into Equations (23) and (24) at the edges of the boundary at $r = r_f$ and $r = r_i$.

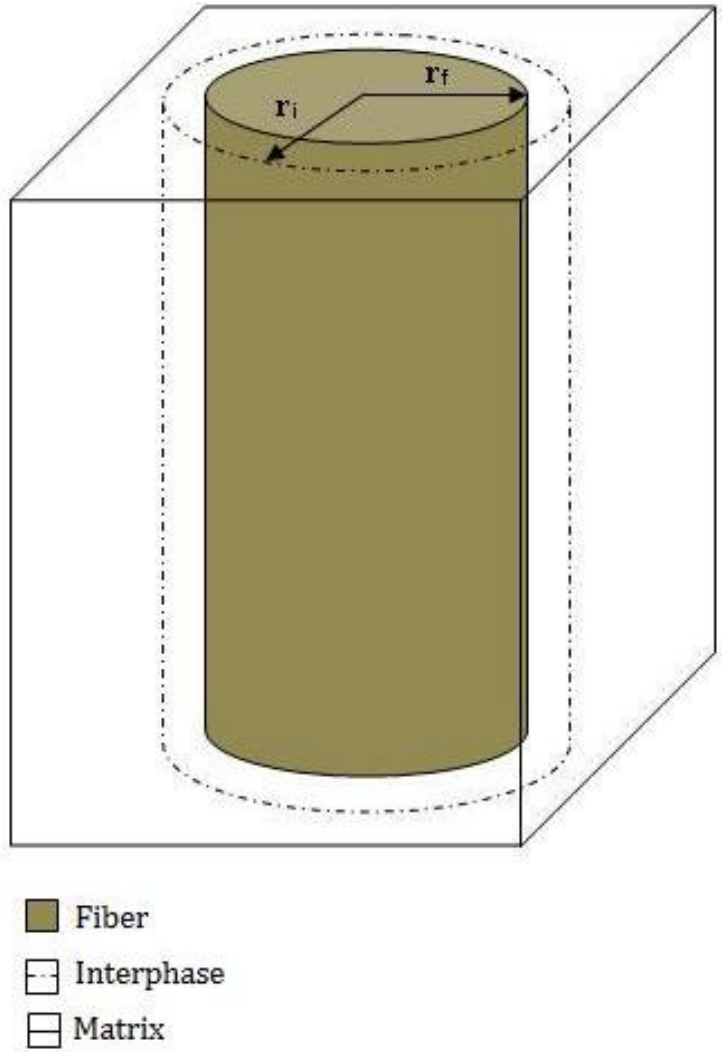

Figure 6 – Schematic Diagram of the Fiber-Interphase-Matrix Composite Model

As mentioned previously, a nonhomogeneous interphase may be discretized by assuming the region consists of discrete intervals of N subregions and equal annulus thickness t_i. In such a case, the Young's modulus and Poisson's ratio of each interval are formulated by the following expressions:

$$\nu_{i(j)} = \frac{\int_{r_{i(j-1)}}^{r_{i(j)}} \nu(r)dr}{r_{i(j-1)} - r_{i(j)}} \quad \text{, and} \tag{25}$$

$$E_{i(j)} = \frac{\int_{r_{i(j-1)}}^{r_{i(j)}} E(r)dr}{r_{i(j-1)} - r_{i(j)}} \tag{26}$$

where $\nu_{i(j)}$ is the Poisson's Ratio of the jth sublayer of the interphase, and $E_{i(j)}$ is the Young's modulus of the jth sublayer of the interphase. Additionally, j = 2,…, n, n+1 and i is the subscript for the interphase. Note that j = 2 denotes the first sublayer of the interphase following the fiber, and j = n+1 denotes the matrix phase.

Several studies have been performed to determine interphase thickness. As pointed out by Gohil and Shaikh [10], it has been observed from literature that the maximum interphase thickness of fiber reinforced composites is up to 10-13% of the fiber radius. In view of the observed measurements Gohil [10] defined the parameter

$$a = \frac{t_i}{r_f} \tag{27}$$

where $0.01 \leq a \leq 0.15$. Here the parameter a in Equation (27) is the ratio of interphase thickness-to-fiber radius.

1.3.1 Sutcu Model

Sutcu [3] developed a recursive concentric cylinder model for predicting the transverse shear modulus G_{23} for continuous, uniaxially aligned fibers with multiple

homogeneous interphases. Each interphase layer is approached as an annular cylinder (also called hollow cylinder), with the fiber being the innermost cylinder. The basic approach begins with the innermost two cylinders, and then replacing the interphase and the fiber assembly with an equivalent homogeneous solid cylinder at each step. The effective elastic properties are then calculated utilizing the Christensen approximation for G_{23}, as governed by Equation (15). This process is repeated until all interphase layers (including the matrix) are incorporated into one homogeneous medium. Figure 7 shows a visual representation of the Sutcu model.

The expression provided by Sutcu [3] and derived from the Christensen [2] Equation (15) for the effective transverse shear modulus is:

$$\bar{G}_{23,j} = G_{23,j} \frac{(B + \sqrt{B^2 - AC})}{(-A)} \tag{28}$$

where $\bar{G}_{23,j}$ is the effective transverse shear modulus of the composite cylinder up to and including the jth sub-layer, where j = 2,…,n, n+1, and j = 2 is the first sublayer following the fiber as is seen in Figure 7, and j = n+1 denotes the matrix phase. $G_{23,j}$ is the modulus of the isotropic constituent phase being replaced. As was the case with the Christensen model, A, B, and C are defined by Equations (16), (17), and (18). Additionally, note that in contrast to the quadratic expression (15) by Christensen, only the physically meaningful root was extracted.

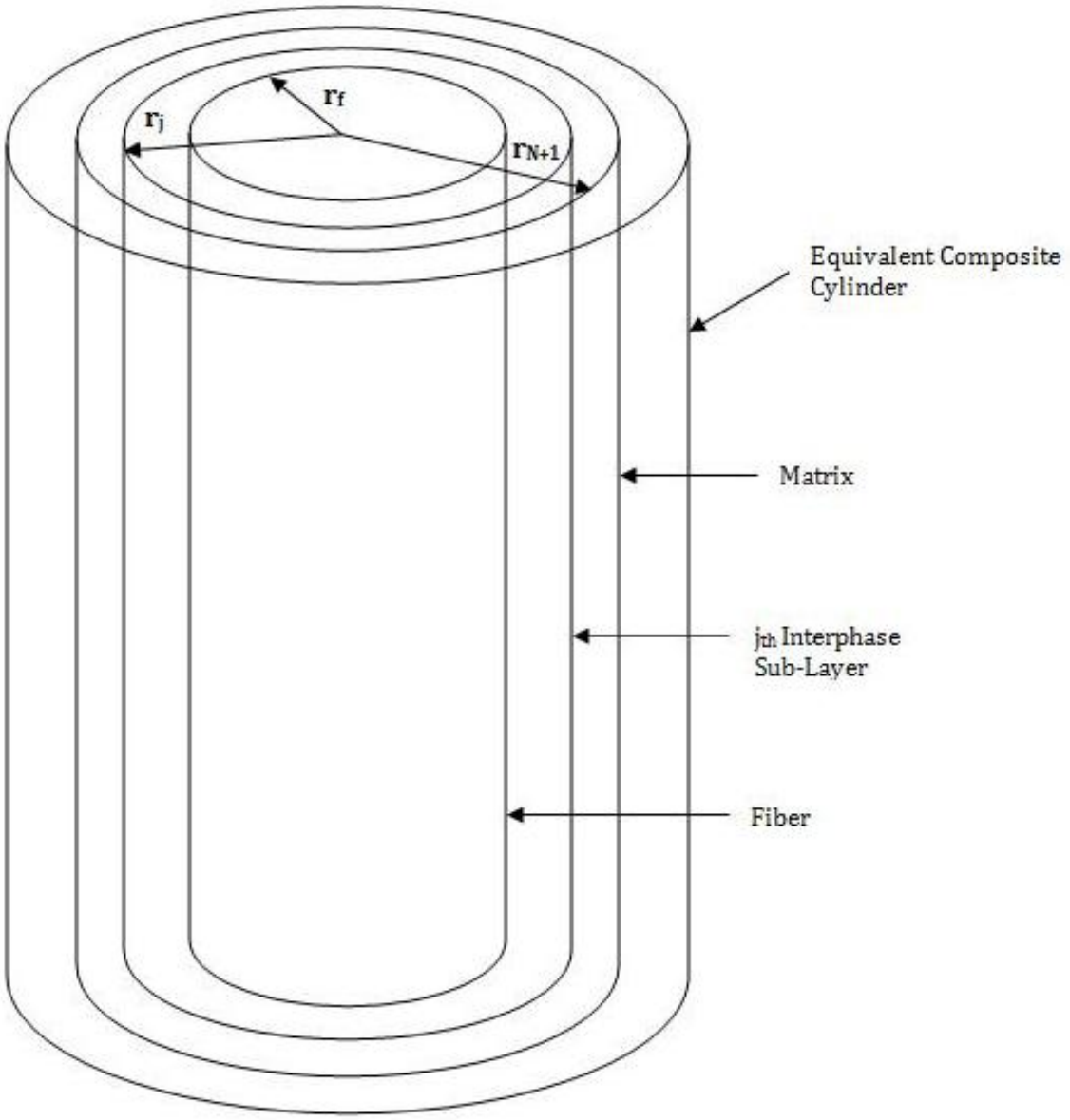

Figure 7 - Sutcu Recursive Concentric Cylinder Model

1.4 Scale Effects of Finite Domain Models

A significant amount of research available in literature [1, 2, 3, 20] makes use of a single RVE embedded in an infinite composite medium. As explained in Sections 1.2.1 – 1.2.2 such RVEs typically consist of a single cylindrical fiber (and

possibly hollow interphase cylinder) embedded in a volumetrically proportionate matrix of specific geometric shape (hollow cylinder, or square cuboid with cylindrical cut-out). Thereafter, effective properties of the RVE are obtained by various analytical models such as the heretofore outlined method. This approach, however, fails to address elastic properties defined in finite domains as the domain size is either increased or decreased. This is specifically relevant to Finite Element Analysis (FEA), as simulation models in this approach utilize models with finite boundaries, which are influenced by these so called scale effects.

The goal of this research is to incorporate considerations of scale effects as it pertains to FEM models that were developed for attaining approximations of the transverse shear modulus of a composite domain. Jiang [21] suggested that the elastic properties depend on the size of the domain of a finite-sized model. The domain as such is called a window and may be placed anywhere in a domain consisting of multiply-bonded composite unit cells. Jiang defined the following parameter as a measure of window size relative to the larger domain:

$$\delta = \frac{L}{d_f} \geq 1 \tag{29}$$

where L denotes the length of a square window, and d_f describes the fiber diameter of the composite RVE. Figure 8 illustrates a window placed over a periodic domain of axially aligned, continuous fibers.

Jiang [21] observed a convergence of elastic properties of a finite domain with uniaxially, aligned cylindrical fibers embedded in a finite matrix medium, subject to displacement and traction boundary conditions (applied separately), when the window size was altered.

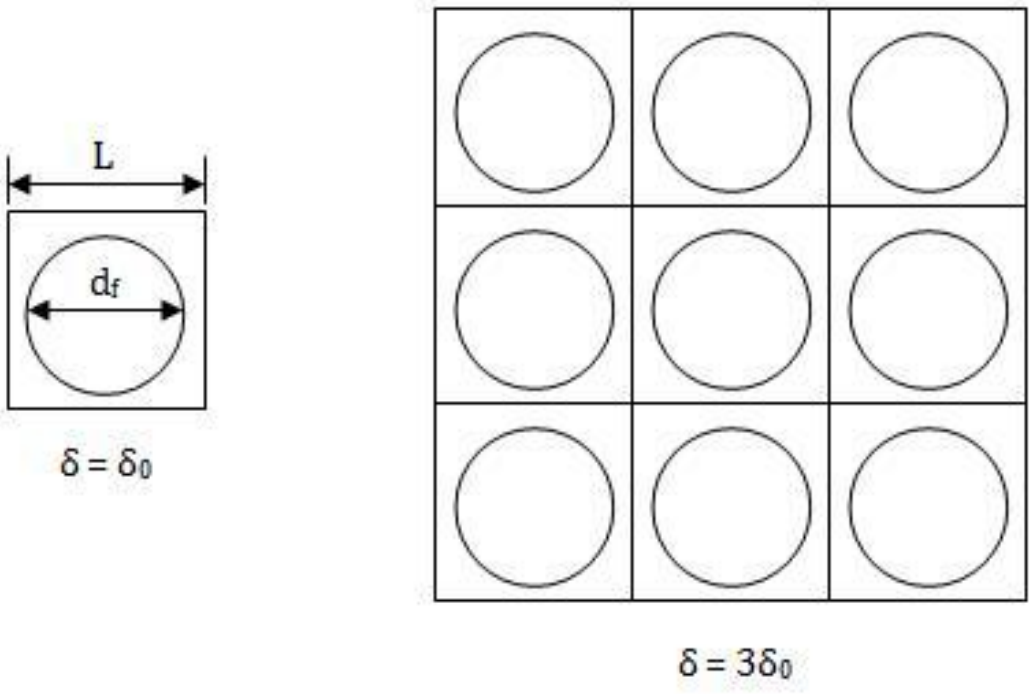

Figure 8 – Window Parameter δ Subject to Varying Scales

Wang [11] studied the effects window size of an FEA model as part of his study of human bone composites, and tabulated results of the numerically derived transverse shear modulus, which indicated a decrease in modulus value with increasing window size, and in conjunction with increasing fiber-to-matrix Young's Modulus ratio, E_f/E_m. Of the parameters studies, the E_f/E_m ratio was observed to have the largest impact on the modulus value. Wang found additionally that fibers located on the boundary of the window accounted for a large difference in apparent elastic moduli.

1.5 Random Transverse Fiber Arrangement

Traditionally, companies and institutions have invested considerably in determining the physical characteristics of fiber reinforced materials through experimental means. Gusev, et. al. [12] described the arrangement of actual composites quite succinctly by stating that reinforced cylindrical fibers in composite sample specimens vary in diameter and shape, and form an "infinite variety of local packing arrangements" [12]. It was therefore stipulated that the aforementioned laboratory samples are statistically homogeneous in the sense that the properties of one sample is indistinguishable from another. Researchers have developed varied micromechanical models [10, 12, 13] that attempt to accurately predict the elastic constants of randomly, transversely arranged, uniaxially-aligned fiber reinforced composites. Through numerical two-dimensional (2-D) FEA simulation, Gusev concluded [12] that random fiber arrangements in a finite domain had a significant influence on the transverse shear modulus, while varying the fiber diameter distribution did not. A calculated average difference in G_{23} of 6.7% was recorded between numerical 2-D models of a periodic and random hexagonal array. Note that the phrase "2-D model" refers to a plane strain assumption.

In a related study, Wang, et. al. [13] developed a procedure to generate a 2-D RVE model based on a randomization of the transverse arrangement of multiply bonded RVEs, with each RVE consisting of a uniaxial fiber embedded in square matrix. The procedure involved translating even (odd) numbered rows (columns) that are originally arranged in a periodic array by a randomly selected increment in a specific coordinate direction. Additional randomization was achieved by translating each fiber by a random increment within the RVE itself. An ensuing study by Wang, et. al. [14] studied the random transverse arrangement of fiber reinforced composites with inclusion of homogeneous interphase. Results indicated a strong

interdependence of interphase properties on the random fiber arrangement of finite domains. In particular, a relatively "weaker stiffening effect is observed" [14] in the transverse Young's modulus of randomly aligned fiber composite models, as the interphase-to-matrix ratio was reduced incrementally from 20, 30, to 40. Thus, Wang concluded that a "reduction in interphase thickness provokes a reduction in the effective modulus of the composites" [14].

1.6 Angular Fiber Misalignment of Uniaxial Continuous Fiber Reinforced Composites

Uniaxially-aligned continuous fibers have been observed to have been misaligned incrementally from their preset fiber direction. Yurgartis [15] measured the angular misalignment of carbon-fiber reinforced aromatic polymer (APC-2) composites and determined that the majority of fibers are oriented within ±3° of the mean fiber direction, having a standard deviation of the sample distribution ranging from 0.693° to 1.936°. Furthermore, 83% of the sample distribution exhibited a fiber inclination within ±1°.

Much debate still exists on the cause of angular fiber misalignment, however, Swift [16] lists several potential causes due to manufacturing processes of continuous fiber composites, such as "machine vibration during filament winding" [16], and "non-uniform curing and cooling shrinkages" [16], among other causes. It is therefore postulated in this thesis that fiber misalignment has a significant influence on the elastic properties of fiber reinforced continuous composites. Further studies [16, 17] reported on the effect of fiber misalignment on the physical properties of short and long fiber composites.

The objectives of this thesis are as follows:

- The purpose of this thesis is to identify and present the state-of-the-art numerical model for determining the transverse shear modulus of aligned, quasi-continuous long-fiber composites.
- Furthermore, this thesis seeks to evaluate the impact of a random distribution of angularly misaligned fibers in uniaxial, continuous fiber reinforced composites on the transverse shear modulus through three-dimensional numerical modeling and evaluation. While studies by Swift [16], Phelps and Tucker [17], and Yurgartis [15] have effectively observed and measured fiber misalignments in short and continuous fiber composites, and have studied possible causes of fiber misalignment [16], this thesis seeks to investigate and evaluate the impact of angular fiber orientation on the transverse shear modulus numerically through the use of three-dimensional FEA models.
- Another objective of this study is to assess the effect of random transverse fiber distribution in uniaxial, continuous fiber reinforced composites on the transverse shear modulus through three-dimensional numerical modeling and evaluation. Previous studies [12, 13] evaluated the impact of random vs. periodic 2-D arrays for fibers with no interphase, and Wang [14] evaluated the impact of random vs. periodic 2-D arrays for fibers with homogeneous interphase.
- Yet a further objective is to gauge the impact of variation of scale effects of periodic and transversely arranged and angularly misaligned random-periodic FEA models on the transverse shear modulus G_{23}. While other studies [11, 21] assessed scale effects on the transverse shear modulus

through numerical modeling of 2-D arrays, this thesis seeks to evaluate the impact of scale effects on G_{23} of 3-D domains.

- Lastly, this thesis seeks to examine the predictive potential of the model developed by Sutcu [3] for composites with interphases, and models by Halpin-Tsai [1] and Christensen [2] for predicting the transverse shear modulus of unidirectional composites without interphases. Previous work by Gusev [12] compared numerical averages to predicted G_{23} values of random and periodic 2-D arrays for fibers with no interphase. In contrast, this study compares numerical averages of 3-D arrays of composites with no interphase, and fibers with homogeneous and nonhomogeneous interphases to predictive models.

CHAPTER 2 FORMULATION

2.1 Finite Element Modeling

The FEA software ANSYS [18] was selected for performing simulations in this study. This program was chosen due to its capability of solving three-dimensional (3-D) linear elasticity problems. The model presented here consists of a 3-D finite domain subjected to displacement loads at its boundaries.

2.2 Geometric Design

The basis of the finite element model is the unit cell, or RVE. Thereafter, an array of cells bound by a domain with finite boundaries consists of multiply-bonded RVEs located in a square arrangement (see Figure 8). In the present study, simulations are developed and executed on single RVEs, as well as multiply-connected RVE cells as periodic and random-periodic arrays, which will be described in more detail in Sections 2.2.1 – 2.2.3. The RVEs developed for the present study are depicted in Figure 9.

Figure 9 depicts a fiber reinforced composite consisting of a cylindrical fiber embedded in a square cuboid matrix (Figure 9a), a domain consisting of nine multiply connected RVEs in a square arrangement (Figure 9b), and domain consisting of 25 multiply connected RVEs in a square arrangement (Figure 9c).

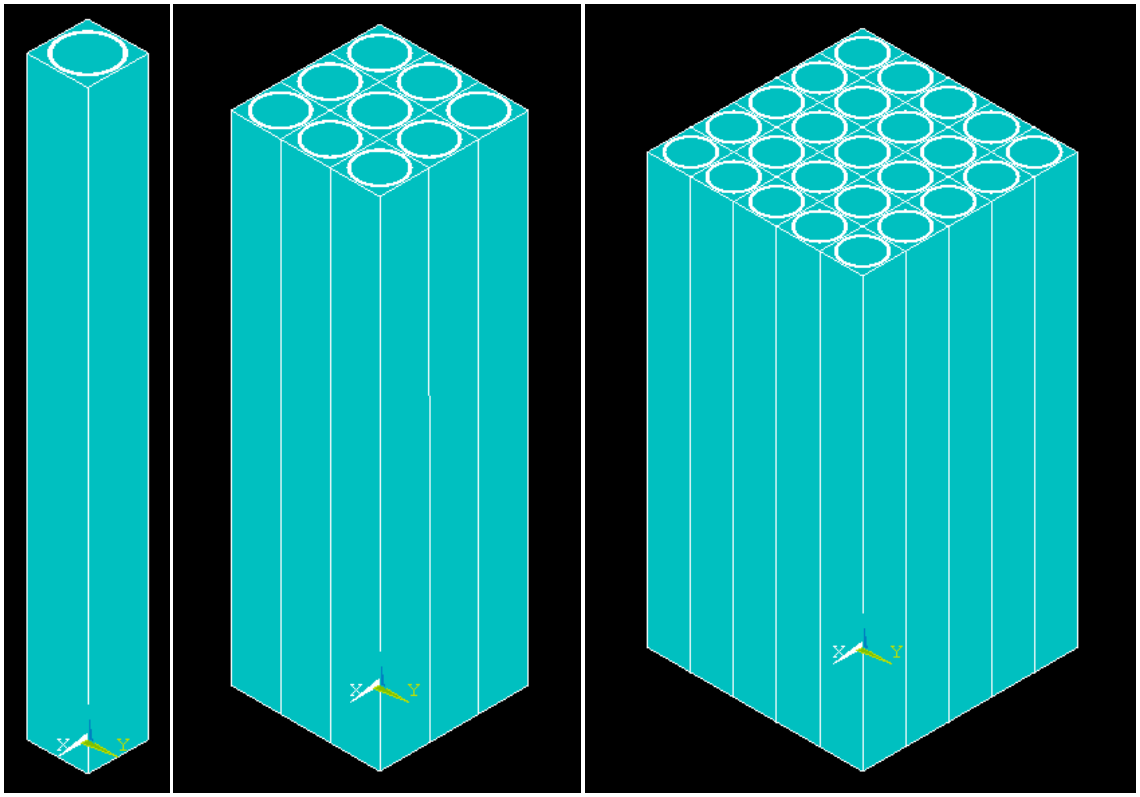

Figure 9 – Finite Element Models Developed in ANSYS. From Left (a) Single RVE, (b) 9-Cell Array, and (c) 25-Cell Array [18]

2.2.1 Periodic Array of Variable Domain Size

The influence of scale and free-edge effects on the elastic properties of composite materials was discussed in chapter 1.4. In view of the findings developed in the studies mentioned therein, multiple models are constructed in this study consisting of arrays of incrementally increasing domain sizes. The same method is employed to achieve varied domain sizes as outlined in Section 1.4. In addition to simulating a single RVE model, a 9-cell (3 x 3) and 25-cell (5 x 5) are designed and constructed as shown in Figure 9. The respective domain-to-fiber diameter ratios are:

$$\delta_{1-\text{Cell}} = \delta_0 \tag{30}$$

$$\delta_{9-\text{Cell}} = 3\delta_0 \tag{31}$$

$$\delta_{25-\text{Cell}} = 5\delta_0 \tag{32}$$

Each multi-cell model consists of perfectly bonded RVEs that are arranged in a square array (Figure 9). The purpose of the design of the aforementioned three-dimensional models is to study the influence of scale and free-edge effect on the transverse shear modulus.

2.2.1.1 Inclusion of Mesoscale Window

In addition to studying the transverse shear modulus over the entire domain volume, the volumetrically averaged transverse shear modulus is evaluated over a centrically isolated mesoscale window, which is the size of a single RVE and is located in the center of the 9-cell and 25-cell model, respectively. A functional schematic thereof is illustrated in Figure 10.

The goal of this procedure is to further study the influence of the free-edge effect on the transverse shear modulus by evaluating a single, isolated RVE that is not subject to any free surface, as well as to study the effect of the shear modulus value with increasing distance from the free edges of the domain.

2.2.2 Transversely Random-Periodic Array of Variable Domain Size

The models introduced up this conjuncture describe solely a periodic array consisting of multiply-connected RVEs. In the preceding arrangement, each RVE is considered in perfect uniaxial alignment along the longitudinal axis, and each fiber is centrically located within each individual matrix cuboid (see Figure 8). In contrast, consider the case in which the fiber or the fiber-interphase composite cylinder is

shifted a discrete random increment in the transverse plane. Figure 11 illustrates the foregoing concept schematically.

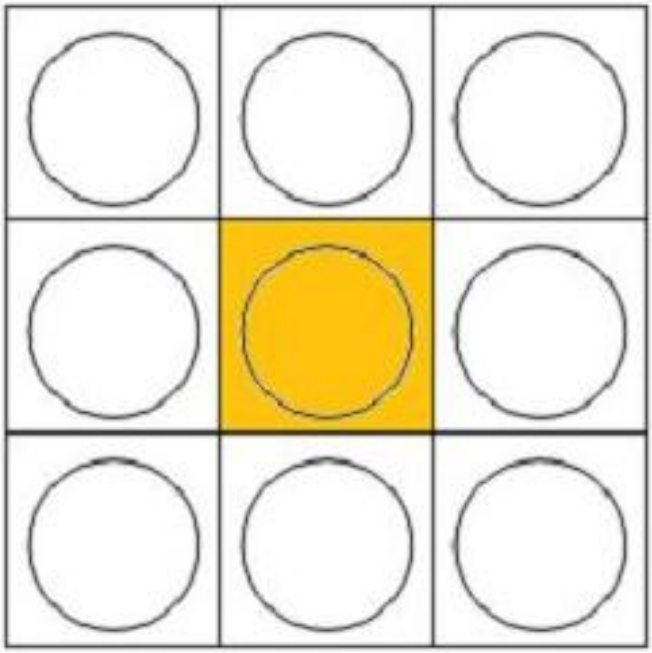

Figure 10 – Centrically Isolated Mesoscale Window of a 9-Cell Domain

In this case, the fiber (fiber-interphase) is translated a random distance in both the x and y direction according to the relation

$$\Delta x_{Fiber} = x_0 + k \cdot c_1 \tag{33}$$

$$\Delta y_{Fiber} = y_0 + k \cdot c_2 \tag{34}$$

where Δx_{Fiber} and Δy_{Fiber} denote the transverse translation of the fiber center in the x and y direction, respectively, x_0 and y_0 describe the initial fiber location, k is a random number ranging from -10 to 10, and c_1 and c_2 are arbitrary constants.

Translation increments vary from zero to a location very near the edge of the matrix. The translation distance limit was set at a point in the plane beyond which topological degeneracy of the model is detected by ANSYS. That is, two keypoints (points that outline the shape of a volume), one describing the contour of the matrix at a point , the other the contour of the fiber, can no longer be analyzed numerically as two separate keypoints by ANSYS due to their relative proximity. Therefore, the cylindrical inclusion is randomly rearranged in the transverse plane from its default centric location to a point right near the edge of the square matrix.

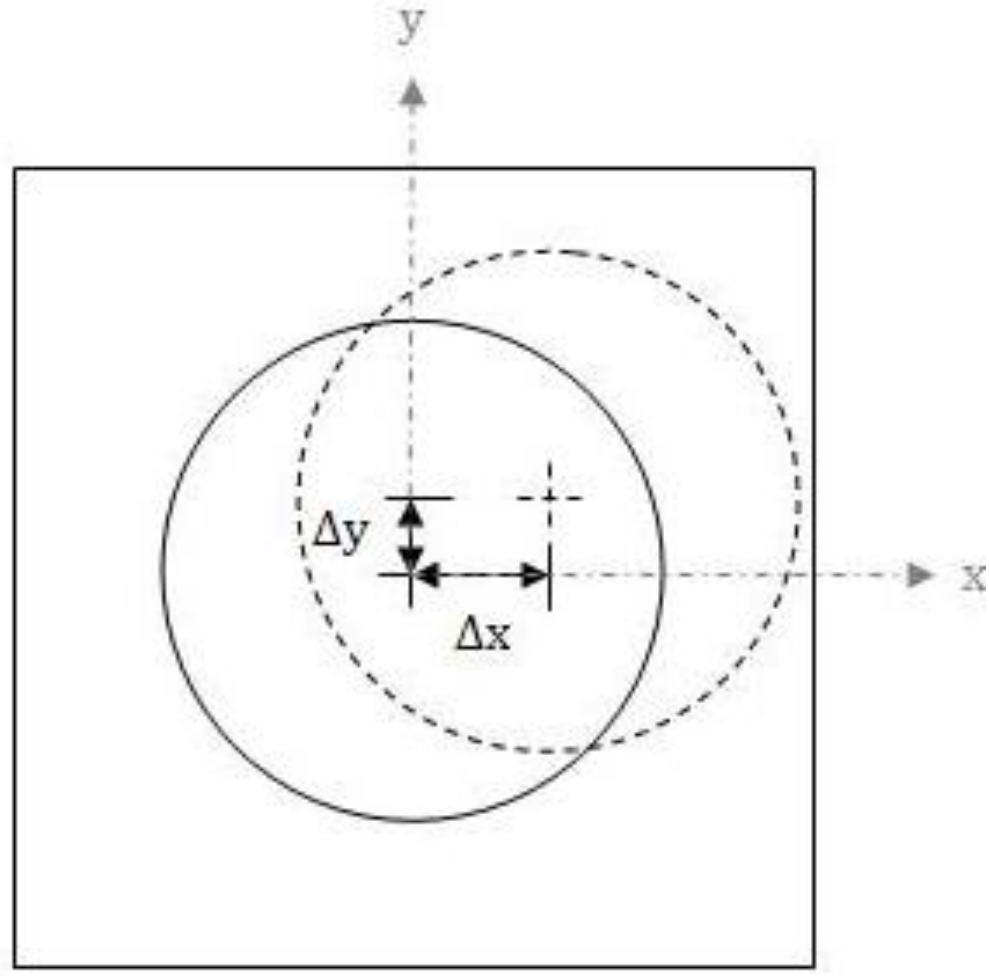

Figure 11 – Incremental Fiber Translation in the Transverse Plane of an RVE

2.2.3 Angular Random-Periodic Array

Similarly to moving the cylindrical inclusions transversely along a plane, the following model developed allows angular rotation of fibers in three dimensions within the boundaries of the square cuboid RVE, as is displayed schematically in Figure 12.

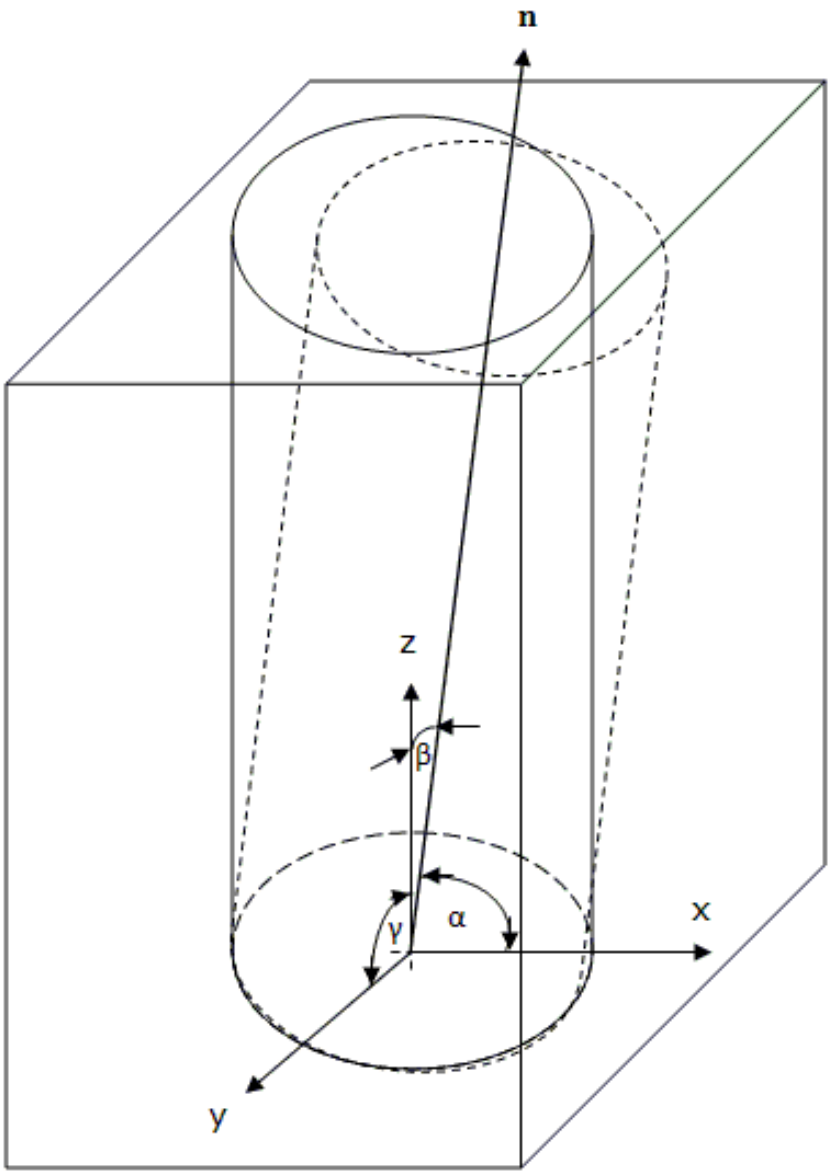

Figure 12 – Angular Fiber Rotations in Three Dimensions Within the RVE

Here, the center of the cylindrical inclusion is hinged at the intersection with the lower transverse boundary plane and rotated by random angular increments about the x, y, and z global axes of the RVE, respectively. The term n denotes the unit normal of the plane perpendicular to the inclined fiber. Each cylindrical inclusion is rotated about each respective axis according to the relations:

$$\Delta\alpha_{Fiber} = k \cdot c_3 \tag{35}$$

$$\Delta\beta_{Fiber} = k \cdot c_4 \tag{36}$$

$$\Delta\gamma_{Fiber} = k \cdot c_5 \tag{37}$$

where k denotes a random number ranging from -10 to 10, and c_3, c_4, and c_5 are arbitrary constants. Rotation increments vary from zero to any point very near the boundary of the RVE. The angular rotation limit is determined due to the aforementioned onset of topological degeneracy of the model.

In the model presented here, the maximum misalignment angle is 0.143°. However, as mentioned in Section 1.6 of this study, previous literature [15] suggests a misalignment range of ±3° for long, axially aligned fiber reinforced composites, whereby 83% of the sample distribution was observed to vary between ±1°. Unfortunately, limitations of the present model do not allow for any fiber rotation past 0.143° due to the aforesaid degeneracy effects in ANSYS. Furthermore, the randomization technique does not follow the sample distribution curve. That is to say, a random number is equally weighted in its probability of being selected out of a pre-determined range of integers, in lieu of employing a randomization procedure that is in accordance with the sample distribution curve (i.e. 83% of all random numbers drawn will equate to an angle within ±1°, etc.).

2.3 Meshing of Geometry

As outlined in the previous section, multiple models are developed for load simulation in ANSYS [18]. All models are meshed using element Solid185, which is used for modeling of 3-D structures. Solid185, shown in Figure 13, is comprised of eight nodes at its corners, each node having three degrees of freedom in the x, y, and z directions.

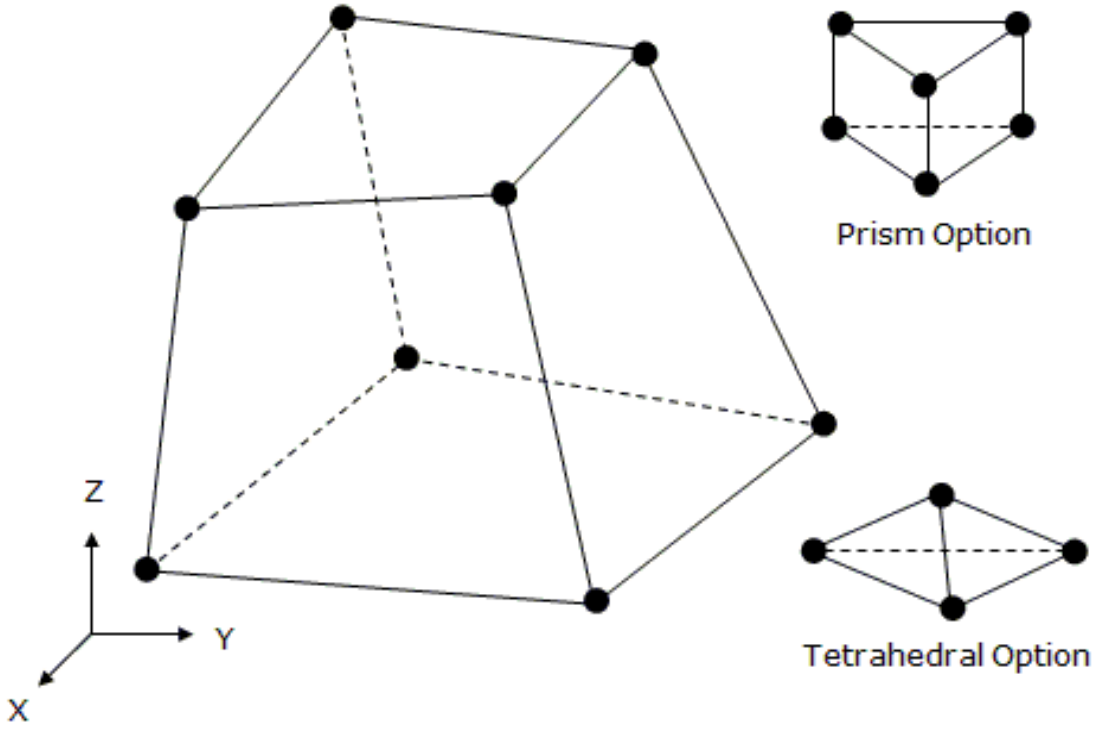

Figure 13 – Schematic Representation of ANSYS Element SOLID185 [18]

While the element has "plasticity, hyperelasticity, stress stiffening, large deflection and large deflection responses" [18], all simulations executed in this thesis assume linear elastic behavior.

2.3.1 Contact Surface Bonding

The surface areas of all models between fiber, interphase, and matrix are considered perfectly bonded for the purpose of this study. The bonding method involves merging of coincident keypoints of neighboring volumes. The ANSYS merge command, termed NUMMRG, is issued for merging separate but coincident components of a model together.

2.4 Material Properties

2.4.1 Fiber and Matrix

The material chosen for this study is a glass/epoxy composite consisting of glass reinforcement fibers and an epoxy matrix. The two elastic moduli required for conducting linear elastic analysis (excluding thermal) of isotropic, homogeneous constituents are Young's modulus E and Poisson's ratio ν. Values for E and ν for both fiber and matrix are extracted from literature [19] and tabulated as follows.

Table 1 – Fiber and Matrix Isotropic Elastic Moduli [19]

Material	**Young's Modulus, E (GPa)**	**Poisson's Ratio, ν**
Glass Fiber	85	0.2
Epoxy Matrix	3.4	0.3

In addition, it should be noted that the volumetric fraction of fiber to matrix used for this study is $V_f = 0.55$. This fiber volume fraction was chosen due to its closeness to actual measured fiber volume fractions from literature [12]. Gusev [12] reported a measured nominal fiber volume fraction of $V_f = 0.54 \pm 0.01$. Glass/Epoxy

was selected as the composite material because both constituent materials are isotropic and thus lend itself well to numerical analysis, as well due to its widespread use in various industries (see [19] for examples).

2.4.2 Interphase

2.4.2.1 Interphase Design

Two separate interphase models are developed for this study. A single homogeneous interphase and a nonhomogeneous interphase consisting of four perfectly bonded homogeneous interphase sublayers are considered. Section 1.3 highlighted commonly selected interphase thicknesses used in related numerical studies. The interphase thickness is a fraction of the fiber radius, and for the purpose of this study, the interphase thickness-to-fiber radius ratio (IFR) for both the homogeneous and non-homogeneous case is related by the respective expressions:

$$IFR_H = \frac{t_i}{r_f} \tag{38}$$

and

$$IFR_{NH} = \frac{t_i}{n \cdot r_f} \tag{39}$$

where t_i and r_f describe the interphase thickness and fiber radius, respectively, and n denotes the number of interphase sublayers. A graphical schematic depicting each interphase model is depicted in Figure 14.

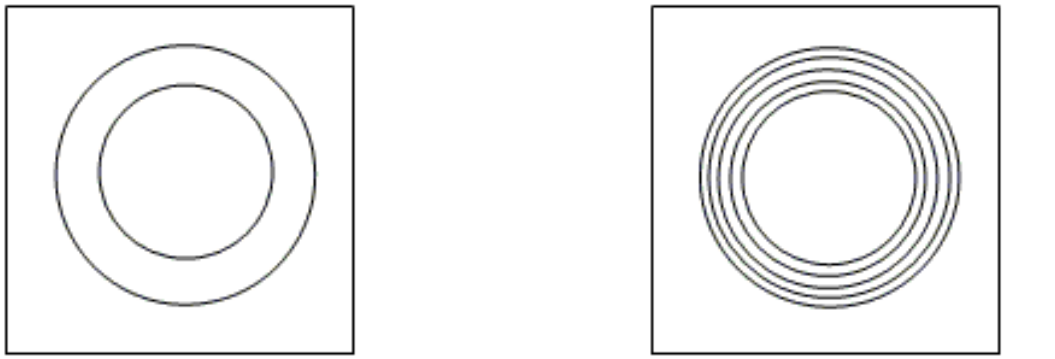

Figure 14 – Interphase Models. From Left (a) Single Homogeneous Interphase and (b) Single Nonhomogeneous Interphase Approximated by Interphase Layers

Thus, it is clear that the interphase sublayers in the case of a four sublayer interphase consist of equal thicknesses t/4. For the present study, an interphase thickness of $t_i = \frac{1}{10} r_f$ is chosen.

2.4.2.2 Interphase Material Properties

The method developed by Garapati [4] as outlined in Section 1.3 for linear variation of Young's modulus and Poisson's ratio is adopted here for determining the properties of both interphase models. Given a linear variation of properties through the radial thickness, the resulting values of E and ν are shown in Table 2.

Table 2 – Interphase Isotropic Elastic Moduli

Interphase Type	Young's Modulus, E (GPa)	Poisson's Ratio, ν
Single Interphase	44.2	0.250
Four-Layer Interphase:		
Layer 1	74.8	0.213
Layer 2	54.4	0.238
Layer 3	34.0	0.263
Layer 4	13.6	0.288

2.5 Boundary Conditions

2.5.1 Volumetric Averaging

To obtain the transverse shear modulus numerically, it is necessary to determine a volumetric average value. In so doing, it is required to establish local stress and strain fields of each element within the domain δ. The concept of strain energy aids in the solution of volumetrically averaged elastic properties, which per Wang [11] is defined as the elastic strain energy stored within the entire body, and is given by the relation

$$U = 1/2 \int_V \sigma_{ij} \cdot \varepsilon_{ij} dV = 1/2 \overline{\sigma_{ij} \cdot \varepsilon_{ij}} \cdot V \qquad (40)$$

where σ_{ij} and ε_{ij} denote stress and strain tensors, respectively, and V describes the volume of the domain. The bar accent denotes volume averages. The average stress and strain can resultantly be written as

$$\overline{\sigma_{ij}} = 1/V \int \sigma_{ij} dV \tag{41}$$

$$\overline{\varepsilon_{ij}} = 1/V \int \varepsilon_{ij} dV \tag{42}$$

It should be pointed out that the stress and strain terms are expressed in tensor notation. Alternatively, the expressions in Equations (41) and (42) may also be written in conventional notation, and may be expressed by the relations:

$$\overline{\tau_{ij}} = 1/V \int \tau_{ij} dV \tag{43}$$

$$\overline{\gamma_{ij}} = 1/V \int \gamma_{ij} dV \tag{44}$$

In terms of finite element formulation, it is evident from Equations (43) and (44) that volume averaging is achieved by summing the stresses and strains in each element, multiplied by the respective element volume according to the relations

$$\overline{\tau_{ij}} = \frac{\sum_{k=1}^{n} (\tau_{ij_k} v_k)}{V} \tag{45}$$

$$\overline{\gamma_{ij}} = \frac{\sum_{k=1}^{n} (\gamma_{ij_k} v_k)}{V} \tag{46}$$

Here, v_k denotes the volume of each element ranging from k = 1, 2,…, n, and n = number of elements.

2.5.2 Displacement Conditions

To compute the apparent elastic transverse shear modulus, homogeneous displacement conditions are imposed on the boundary of the domain as follows:

$$u_2(x) = \varepsilon_{23}^0 \cdot x_2 \tag{47}$$

$$u_3(x) = \varepsilon_{23}^0 \cdot x_3 \tag{48}$$

where ε_{23}^0 represents uniform shear strain (in tensor notation) applied at the boundaries of the domain, as is illustrated in Figure 15. The applied boundary conditions represent a condition of pure shear loading, meaning that all other strain terms at the boundary vanish.

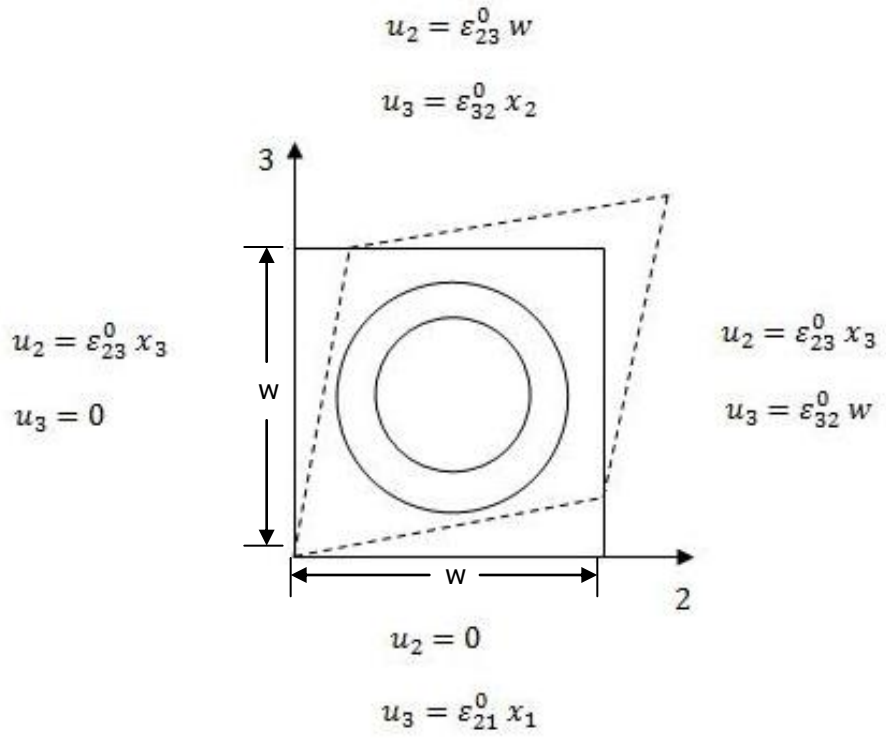

Figure 15 – Single RVE Subject to Pure Shear Displacement Boundary Conditions

Figure 15 shows the top view of a three-dimensional single cell RVE with a fiber, a single interphase, and a square matrix subject to pure shear displacement boundary conditions. The term x_n (n = 2,3) represents the coordinate along the 2 or 3 axis, and w denotes the width of the square matrix.

CHAPTER 3 RESULTS

3.1 Transverse Shear Modulus of a Periodic Array

3.1.1 Effects of Variable Domain Size

As has been characterized in section 2.2.1, a periodic model consisting of cylindrical fibers embedded in square cuboid matrices can be represented with repeating RVEs, where each RVE is the smallest characteristic volume that contains the same material properties and geometry as the entire composite medium. In this section, the apparent transverse modulus G_{23}, obtained by applying boundary conditions, was observed to deviate when the domain size is increased from a single RVE unit cell to 9-cell domain, and finally a 25-cell array. Further distinction was made between interphase types of each domain. Volume averages were determined for domains with no interphase, homogeneous interphase, and with nonhomogeneous interphase. In addition, percentage differences between numerically determined transverse shear modulus averages and G_{23} values predicted with Sutcu's model were evaluated.

This study should provide insight into understanding the importance of domain size selection in numerical finite element analysis as it pertains to 3-D models. Illustrated in Figure 16 is a 25-cell domain subject to pure shear deformation. The graphical representation by ANSYS depicts the deformed body (shown in blue) as well as the undeformed edges prior to application of loads (dashed lines).

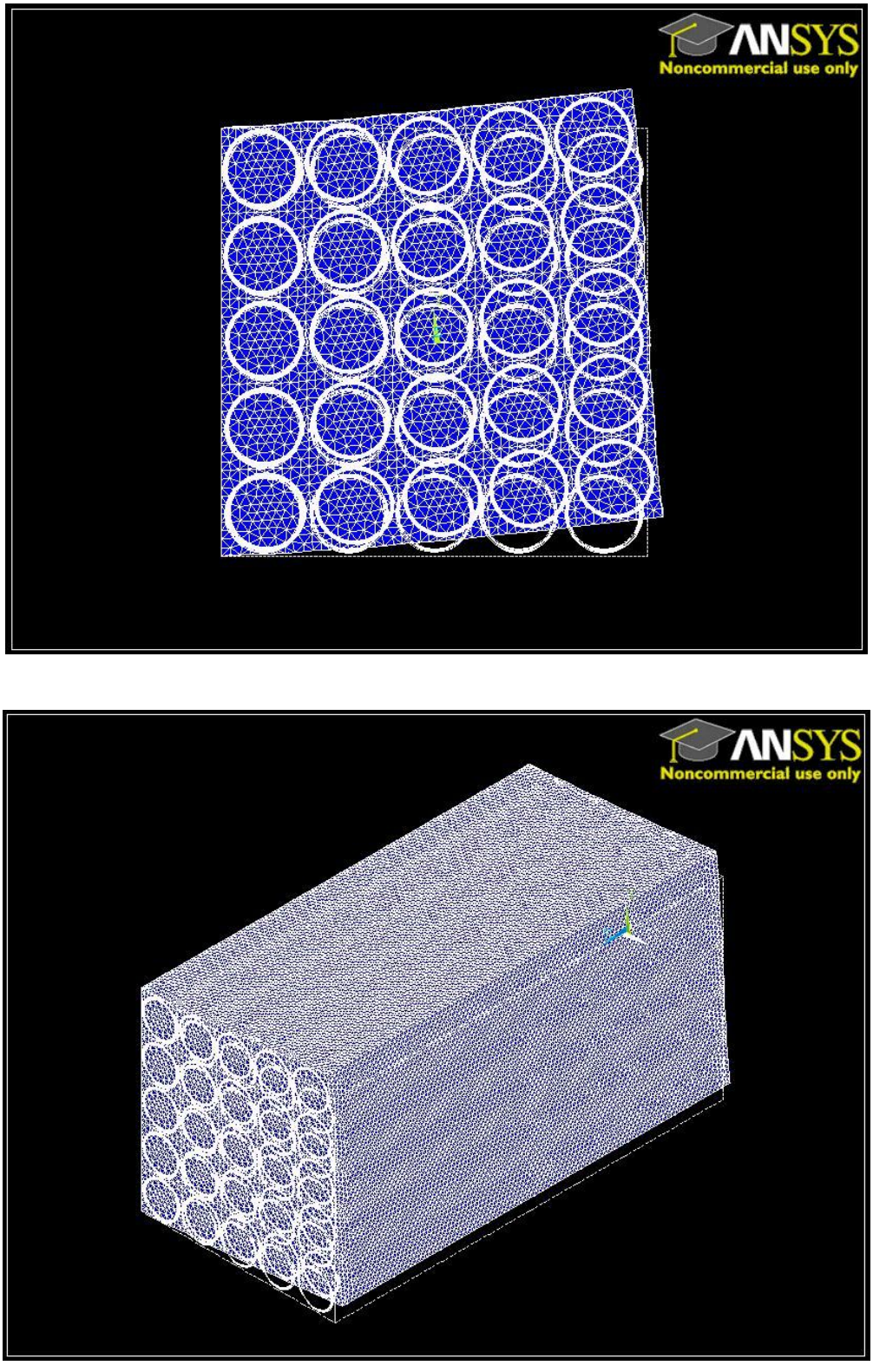

Figure 16 – FEA Simulation of a 25-Cell Array. From Top (a) Top View of Deformation and (b) Deformation in 3-D Isometric View [18]

Subsequent numerical analysis yielded the following results.

Table 3 - Volumetrically Averaged Transverse Shear Modulus G_{23} of Periodic Array Models

Interphase Type	Domain Size	G_{23} [GPa]	|%Δ|*
No Interphase	1-cell	4.364	-
	9-cell	3.361	29.8
	25-cell	3.284	2.3
Homogeneous Interphase	1-cell	6.025	-
	9-cell	4.524	33.2
	25-cell	4.408	2.6
Nonhomogeneous Interphase	1-cell	5.920	-
	9-cell	4.436	33.5
	25-cell	4.322	2.6

*Percentage difference with Sutcu Model.

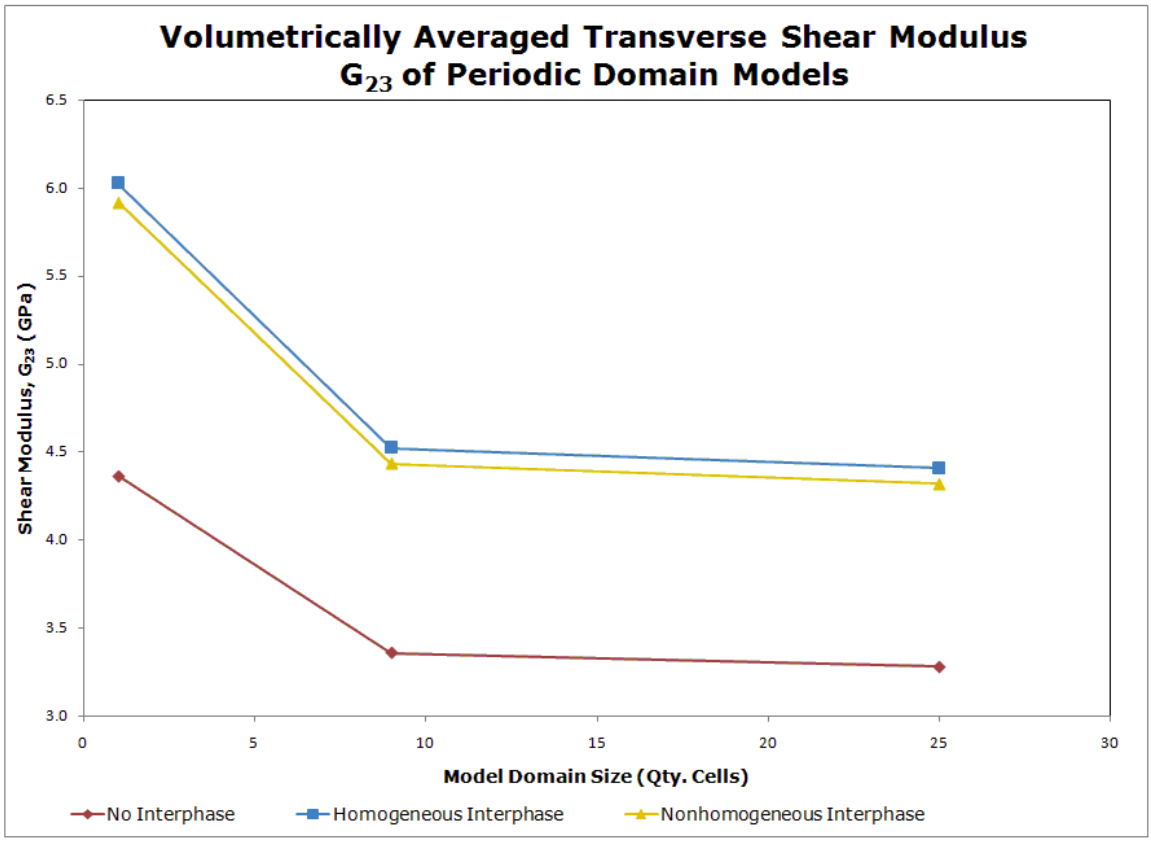

Figure 17 – Volumetrically Averaged Transverse Shear Modulus G_{23} of Periodic Domain Models

All three array configurations exhibit a decrease in moduli with incrementally increasing domain size. Table 3 indicates a significant drop off from the single cell RVE to the 9-cell domain. Figure 17 indicates a convergent response as domain size is continually increased, as the slope of the curve lessens.

3.1.2 Effects of Centrically Isolated Mesoscale Window

The impact of calculating the volumetric averages of a centrically isolated mesoscale window on the transverse shear modulus was evaluated.

Table 4 - Volumetrically Averaged Transverse Shear Modulus of Centrically Isolated Mesoscale Window of Periodic Array Models

Interphase Type	Domain Size	G_{23} [GPa]	$\lvert\%\Delta\rvert_{\text{Complete Domain vs. Window}}$
No Interphase	1-cell	4.364	0.0
	9-cell	3.349	0.4
	25-cell	3.258	0.8
Homogeneous Interphase	1-cell	6.025	0.0
	9-cell	4.510	0.3
	25-cell	4.368	0.9
Nonhomogeneous Interphase	1-cell	5.920	0.0
	9-cell	4.423	0.3
	25-cell	4.283	0.9

Table 4 compares the percentile change in modulus values, obtained by calculating the volumetric averages over the entire domain volume as compared to numeric averages of the center RVE volume (of the same domain) only. The results

indicate a marginal increase in moduli with all simulated scenarios. The effect of isolating the center unit cell appears to be less profound than altering domain size.

3.2 Transverse Shear Modulus of Random-Periodic Arrays

3.2.1 Transversely Random Arrangements

In light of the findings presented thus far, it is of interest to investigate the effect of transversely random-periodic fiber arrangements on the transverse shear modulus. Gusev [12] shows SEM micrographs of glass/epoxy composites that revealed a random distribution of fibers in the transverse plane. Subsequent numerical simulations showed a significant sensitivity in the value of G_{23} (deviation of 6.7% between numerical models of a periodic vs. random array). However, the FEA model used by Gusev was two-dimensional under plane strain conditions. The results presented in Figure 18 and Table 5 that follow represent a 3-D model, and the cylindrical inclusions of which are considered to be quasi-continuous long-fibers with a fiber length-to-matrix width ratio of 10:1.

Table 5 - Volumetrically Averaged Transverse Shear Modulus G_{23} of Transverse Random-Periodic Array Models

Interphase Type	Domain Size	G_{23} [GPa]	$\lvert\%\Delta\rvert_{\text{Periodic vs. Random}}$
Nonhomogeneous Interphase	1-cell	6.063	2.4
	9-cell	4.711	5.8
	25-cell	4.388	1.5

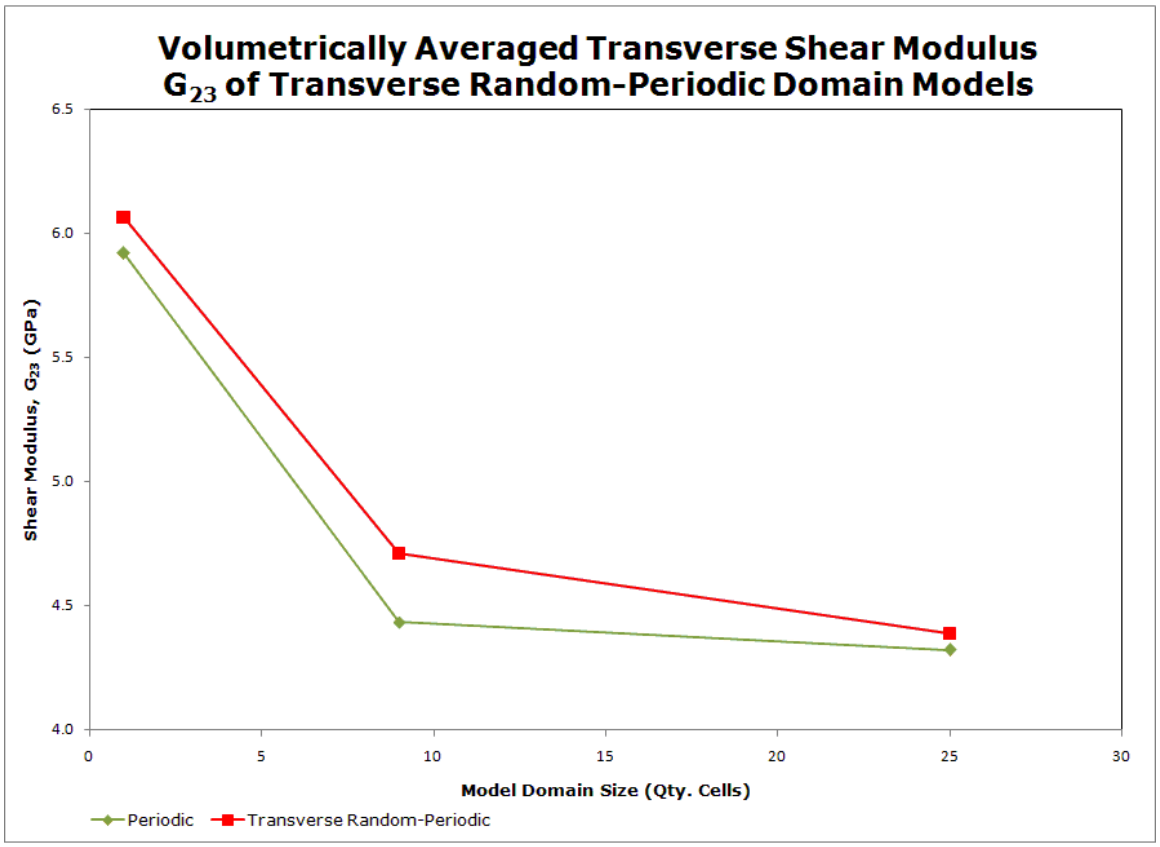

Figure 18 - Volumetrically Averaged Transverse Shear Modulus G_{23} of Transverse Random-Periodic Array Models

The results indicate a moderate variation in stiffness when compared to a periodic model of equal domain size. A maximum deviation of 5.8% was detected for the 9-cell model. Moreover, the data indicates an extenuation in the sensitivity of the response with domain expansion as the percent difference dwindles to a mere 1.5% for the 25-cell array.

3.2.2 Angular Random Arrangements

Section 1.6 summarized research studies which indicated the existence of slight angular misalignments of uniaxial, aligned fiber reinforcements in composites. Gusev [12] observed misalignment angles of ±1° of 83% of a Carbon-APC composite

sample distribution. The volumetrically averaged G_{23} values of randomly misaligned fibers of angles up to ±0.143° are given in the data set that follows.

Table 6 - Volumetrically Averaged Transverse Shear Modulus G_{23} of Angular Random-Periodic Array Models

Interphase Type	Domain Size	G_{23} [GPa]	$\lvert\%\Delta\rvert_{\text{Periodic vs. Random}}$
Nonhomogeneous Interphase	1-cell	5.927	0.1
	9-cell	4.419	0.4
	25-cell	4.334	0.3

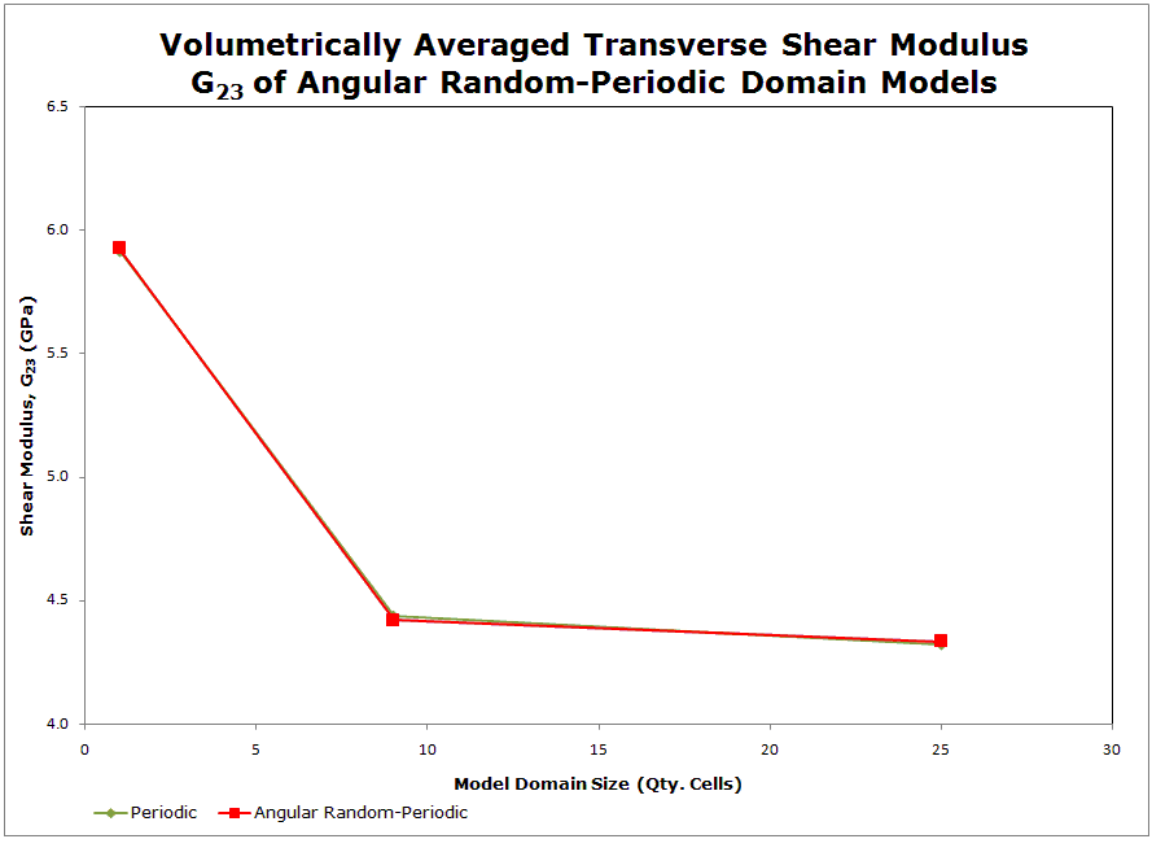

Figure 19 - Volumetrically Averaged Transverse Shear Modulus G_{23} of Angular Random-Periodic Array Models

The findings indicate marginal sensitivity toward the shear modulus, which is expected given the small degree of change in polar fiber orientation. A maximum deviation of 0.4% was detected for the 9-cell model. Similarly to the transverse random-periodic domain simulations, the data indicates an extenuation in the sensitivity of the response with domain expansion as the percent difference dwindles to a mere 0.3% for the 25-cell array.

3.3 Comparison with Theoretical Approximations

Table 7 lists predictions of three micromechanical models introduced in this report (Halpin-Tsai [1], Christensen [2], and Sutcu [3]).

Table 7 - Transverse Shear Modulus G_{23} of Common Predictive Models

Volume Averages of Periodic Arrays					
Interphase Type	**Domain Size**	**Domain Scale**	**G_{23} [GPa]**		
			Current Model	**Christensen /Sutcu*[1]**	**Halpin-Tsai**
No Interphase	25	Center Cell	3.258	3.807 (14.4%)*[2]	3.504 (7%)*[2]
Homogeneous Interphase	25	Center Cell	4.368	4.560 (4.2%)*[2]	-
Nonhomogeneous Interphase	25	Center Cell	4.283	4.437 (3.5%)*[2]	-

*[1] Sutcu model and Christensen model are identical for composites with no interphase. Homogeneous and nonhomogeneous models are approximated by Sutcu model.

*[2] Reflects absolute percent difference from current model G_{23} value.

3.3.1 Fiber-Matrix Predictive Models

Predictive models by Halpin-Tsai and Christensen describe the elastic response of a single fiber embedded in a cylindrical matrix. Results indicate good agreement with the Halpin-Tsai approximation. The numerical average for a 25-cell model is within 7% of the predicted result. The Christensen model is in lesser agreement with the volumetric averages, but still reflects a moderate closeness within 14.3%.

3.3.2 Fiber-Interphase-Matrix Predictive Models

Listed in Table 7 are predictions by Sutcu's approximation for cylindrical fibers surrounded by a homogeneous interphase layer, as well as for fibers surrounded by a nonhomogeneous interphase, respectively, embedded in a cylindrical matrix. Numerical results show excellent agreement with predicted values of G_{23}. The homogeneous interphase model is within 4.2% of Sutcu's result and shows convergent behavior with incremental augmentation of interphase layers, as the nonhomogeneous shear modulus is within 3.5% Sutcu's value.

CHAPTER 4 – CONCLUSIONS

The purpose of this study was to identify and present the state-of-the-art numerical model for determining the transverse shear modulus of aligned, quasi-continuous long-fiber glass/epoxy composites. A further objective was the evaluation of the impact of variation of scale effects of periodic, and transversely arranged and angularly misaligned random-periodic, FEA models on the transverse shear modulus G_{23}. Lastly, this study examined the predictive potential of the model developed by Sutcu [3] for composites with interphases, and models by Halpin-Tsai [1] and Christensen [2] for predicting the transverse shear modulus of unidirectional composites without interphases.

The findings and conclusions are as follows:

- Among the models simulated, the Halpin-Tsai approximation displayed good agreement with volumetric averages determined numerically from a 25-cell three-dimensional periodic array consisting of fiber-matrix RVEs. The numerical average for a 25-cell model is within 7% of the current model. It must be emphasized, however, that the Halpin-Tsai model is dependent on the reinforcement factor ζ, which varies according to geometric cross-section and orientation of the fiber within the matrix. In this study, the reinforcement factor for a cylindrical fiber arranged in a square array was chosen. The Christensen and Sutcu models, on the other hand, are independent of such geometric factors and packing arrangements. The Christensen model gives reasonably close results

- (14.3% within the current model) as well; however, the predicted value is in less relative proximity as compared to Halpin-Tsai's results. Sutcu's predictive model shows excellent agreement with FEA models containing fibers with interphase layers. A convergence in proximity was observed with piecewise extension of the interphase layers.
- An increase in domain size was observed to significantly curtail stiffness averages. Modulus values were found to decrease in a convergent manner with increasing domain size. G_{23} values dropped 33.5% from the nonhomogeneous single cell to the 9-cell model, and 2.6% from the 9-cell array to the 25-cell model.
- The effect of mesoscale window proved to influence the modulus only marginally in conjuncture with incremental increase in domain size. Numerical averages of the complete 9-cell domain deviated only 0.3% from the G_{23} value of the centrically isolated RVE within the same 9-cell domain. The percent deviation was observed to increase marginally with increasing domain size. However, the effect of a mesoscale window was yet relatively insignificant for the 25-cell domain with a difference of only 0.9%.
- Simulations involving the transverse translation of random-periodic arrays were found to affect modulus values. However, the impact was seen to diminish with increasing domain size. For random transverse distribution of fibers, a difference in modulus of +1.5% was observed for the 25-cell array as compared a periodic array of equal size.
- Values of G_{23} for fiber reinforced composite arrays subject to random fiber misalignments revealed a marginal increase in transverse stiffness for random-periodic domains with inclination angles up to ±0.143°. A deviation of +0.3% was predicted for 25-cell arrays subject to random

angular fiber misalignments as compared 25-cell periodic arrays. Similarly to transverse random-periodic array simulations, the results indicate a diminishing influence of fiber misalignment on values of G_{23} with increasing domain size. Both transversely arranged and angular random-periodic models showed excellent agreement with Sutcu's predictive model for composites comprising fiber-matrix models incorporating a nonhomogeneous interphase. Consequently, in as much the random-periodic arrangements studied are deemed to affect the shear modulus averages moderately for 25-cell domains, deviations are nonetheless in close concurrence with Sutcu's results.

REFERENCES

[1] J. C. Halpin and J. L. Kardos, "The Halpin-Tsai Equations: A Review," *Polymer Engineering and Science*, vol. 16, no. 5, pp. 344-352, 1976.

[2] R. M. Christensen and K. H. Lo, "Solutions for Effective Shear Properties in Three Phase Sphere and Cylinder Models," *Journal of Mechanics and Physics of Solids*," vol. 27, no. 4, pp. 315-330, 1979.

[3] M. Sutcu, "A Recursive Concentric Cylinder Model for Composites Containing Coated Fibers," *International Journal of Solids and Structures*, vol. 29, no. 2, pp. 197-213, 1992.

[4] S. H. Garapati, "Effect of Geometry, Loading and Elastic Moduli on Critical Parameters in a Nanoindentation Test in Polymeric Matrix Composites with a Nonhomogeneous Interphase," *Composite Interfaces*, vol. 18, no. 3, pp. 275-294, 2011.

[5] J. M. Whitney and R. L. McCullough, *Micromechanical Materials Modeling*. Delaware: Taylor and Francis, Inc., 1990.

[6] F. Delale and F. Erdogan, "On the Mechanical Modeling of the Interfacial Region in Bonded Half-Planes," *Journal of Applied Mechanics*, vol. 55, no. 2, pp. 317-323, 1988.

[7] F. Erdogan, "Fracture Mechanics of Functionally Graded Materials," *Composites Engineering*, vol. 5, no. 7, pp. 753-770, 1995.

[8] A. Kaw, K. Selvarathinam and G. H. Besterfield, "Comparison of Interphase Models for a Crack in Fiber Reinforced Composite," *Theoretical and Applied Fracture Mechanics*, vol. 17, no. 2, pp. 133-147, 1992.

[9] V. T. Bechel and A. Kaw, "Fracture Mechanics of Composites with Nonhomogeneous Interphases and Nondilute Fiber Volume Fractions," *International Journal of Solids and Structures*, vol. 31, no. 15, pp. 2053-2070, 1994.

[10] P. P. Gohil and A. A. Shaikh, "Analytical Investigation and Comparative Assessment of Interphase Influence on Elastic Behavior of Fiber Reinforced Composites," *Journal of Reinforced Composites*, vol. 29, no. 5, pp. 685-699, 2010.

[11] C. Y. Wang, "Scale and Boundary Condition Effects on Elastic Moduli of Trabecular Bone," M.S. Thesis, Concordia University, AS (ME) Dept., Montreal, 2006.

[12] A. A. Gusev, P. J. Hines, and I. M. Ward, "Fiber Packing and Elastic Properties of a Transversely Random Unidirectional Glass/Epoxy Composite," *Composites Science and Technology*, vol. 60, no. 4, pp. 535-541, 2000.

[13] Z. Wang, X. Wang, J. Zhang, W. Liang and L. Zhou, "Automatic Generation of Random Distribution of Fibers in Long-Fiber-Reinforced Composites and Mesomechanical Simulation," *Materials and Design*, vol. 32, no. 2, pp. 885-891, 2011.

[14] X. Wang, J. Zhang, Z. Wang, S. Zhou, X. Sun, "Effects of Interphase Properties in Unidirectional Fiber Reinforced Composite Materials," *Materials and Design*, vol. 32, no. 6, pp. 3486-3492, 2011.

[15] S.W. Yurgartis, "Measurement of Small Angle Fiber Misalignments in Continuous Fiber Composites," *Composites Science and Technology*, vol. 30, no. 4, pp. 279-293, 1987.

[16] D. G. Swift, "Elastic Moduli of Fibrous Composites Containing Misaligned Fibres," *Journal of Physics*, vol. 8, no. 3, pp. 223-240, 1975.

[17] J. Phelps and C. L. Tucker III, "An Anisotropic Rotary Diffusion Model for Fiber Orientation in Short- and Long-Fiber Thermoplastics," *Journal of Non-Newtonian Fluid Mechanics*, vol. 156, no. 3, pp. 165-176, 2009.

[18] *ANSYS 13.0*. Computer Software. ANSYS, Inc., 2012.

[19] A. K. Kaw, Mechanics of Composite Materials, Second Edition. Boca Raton: CRC Press, 2005.

[20] T. S. Chow and J. J. Hermans, "The Elastic Constants of Fiber Reinforced Materials," vol. 3, no. 3, pp. 382-396, 1969.

[21] M. Jiang, "Scale and Boundary Conditions Effects in Fiber-Reinforced Composites," Ph. D. Dissertation, Georgia Institute of Technology, ME Dept., Atlanta, 2000.

[22] G. Wacker, A. K. Bledzki and A. Chate, "Effect of Interphase on the Transverse Young's Modulus of Glass/Epoxy Composites," *Composites Part A: Applied Science and Manufacturing*, vol. 29, no. 5-6, 619-626, 1998.

[23] Z. Hashin, "Analysis of Composite Materials: A Survey," *Journal of Applied Mechanics*, vol. 50, 481-505, 1983.

[24] R. Hill, "A Self-Consistent Mechanics of Composite Materials," *Journal of the Mechanics and Physics of Solids*, vol. 13, no. 4, 231-222, 1965.

APPENDICES

Appendix A: List of Equations

Appendix A (Continued)

Appendix A (Continued)

Appendix B: Permissions

Figure 9, Figure 13, and Figure 16 are copied figures from or created with the software program ANSYS [18], and are permitted for use and display in this thesis per the written permission that is shown in the e-mail screen shot in Appendix B.

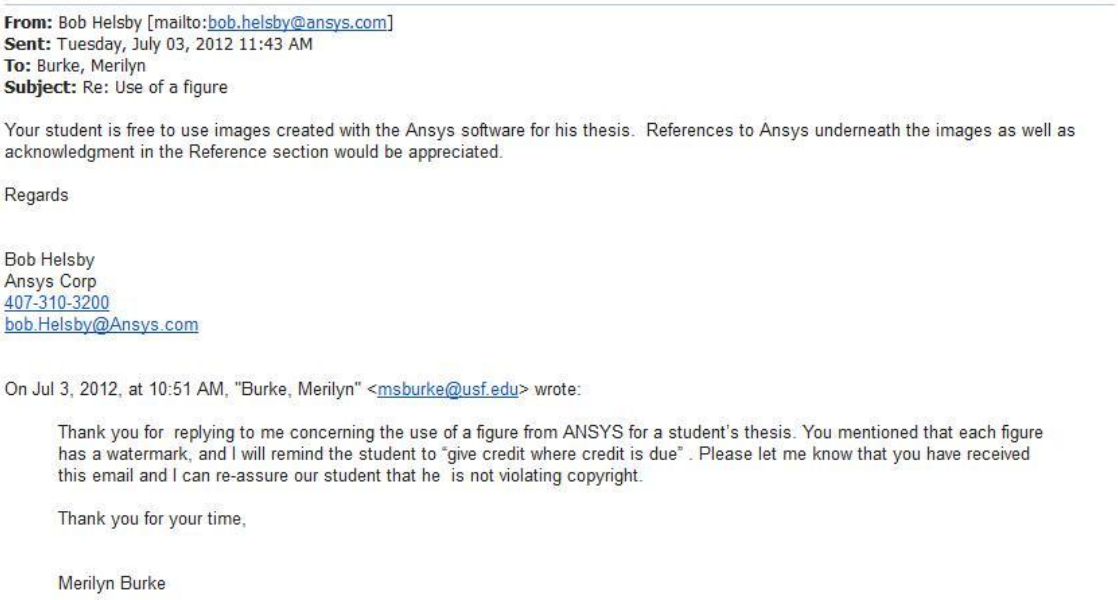

From: Bob Helsby [mailto:bob.helsby@ansys.com]
Sent: Tuesday, July 03, 2012 11:43 AM
To: Burke, Merilyn
Subject: Re: Use of a figure

Your student is free to use images created with the Ansys software for his thesis. References to Ansys underneath the images as well as acknowledgment in the Reference section would be appreciated.

Regards

Bob Helsby
Ansys Corp
407-310-3200
bob.Helsby@Ansys.com

On Jul 3, 2012, at 10:51 AM, "Burke, Merilyn" <msburke@usf.edu> wrote:

> Thank you for replying to me concerning the use of a figure from ANSYS for a student's thesis. You mentioned that each figure has a watermark, and I will remind the student to "give credit where credit is due" . Please let me know that you have received this email and I can re-assure our student that he is not violating copyright.
>
> Thank you for your time,
>
> Merilyn Burke

Figure A1 – ANSYS Copied Figures Permission E-Mail Screen Shot